Aalto University
School of Chemical Engineering
Degree Program of Chemical and Process Engineering

Ekaterina Sakarinen

THERMO-RESPONSIVE CELLULOSE HYDROGELS BY GRAFTING LOW-MOLECULAR-WEIGHT POLYMER CHAINS

Master's Thesis
Espoo, May 10, 2019

Supervisor: Prof. Dr. Mauri Kostiainen, Aalto University
Instructor: Dr. Katja Heise, Aalto University

Aalto University
School of Chemical Engineering
Degree Program of Chemical and Process Engineering

ABSTRACT OF MASTER'S THESIS

Author:	Ekaterina Sakarinen		
Title:	Thermo-responsive cellulose hydrogels by grafting low-molecular-weight polymer chains		
Date:	May 10, 2019	**Pages:**	65
Supervisor:	Prof. Dr. Mauri Kostiainen		
Instructor:	Dr. Katja Heise		

Low-molecular-weight (2.5-10 kDa) thermo-responsive polymers were synthesized through atom transfer radical polymerization (ATRP) and grafted onto carboxymethyl cellulose (CMC) and cellulose nanofibers (CNF) in two different ways. In the first approach, amino-terminated poly(di(ethylene glycol) methyl ether methacrylate) (PDEGMA-NH_2) and poly(*N*-isopropylacrylamide) (PNIPAM-NH_2) were used to produce graft copolymers with CMC and CNF in water by using water-soluble carbodiimide and *N*-hydroxysuccinimide as cross-linkers. In the second approach, click chemistry was employed to cross-link alkyne-modified CMC and CNF with azido-terminated PNIPAM (PNIPAM-N_3) in the presence of a Cu(II) catalyst. For both synthetic approaches, elemental analysis and infrared spectroscopy were used to confirm polymer grafting. Dynamic light scattering (DLS) and UV-VIS spectroscopy measurements proved that the formed hydrogels exhibited thermo-responsive properties. The rheological behavior of the copolymers was evaluated in water at 25 and 50 °C. The obtained thermo-responsive hydrogels based on natural and biocompatible starting materials pave the way for the design of injectable hydrogels to be used in biomedical applications.

Keywords:	cellulose hydrogels, thermo-responsive polymers, modification of polysaccharides, click chemistry, graft copolymers
Language:	English

ACKNOWLEDGEMENTS

My deepest gratitude goes first and foremost to my advisor Dr. Katja Heise for letting this thesis be my own work but steering me in the right direction whenever I needed it. I would also like to thank my supervisor Prof. Dr. Mauri A. Kostiainen for the warm encouragement and constructive advice he has provided me in this thesis process.

I take this opportunity to express gratitude to all other members of BiHy group for their help and support. My special thanks goes to MSc. Antti Korpi for patient guidance and assistance with polymerizations and dynamic light scattering measurements.

I would also like to thank Dr. Jari Koivisto, MSc. Afsoon Farzan and MSc. Panu Noppari for teaching me how to use the characterization instruments. I am also grateful to Kaisa Hytti for determining the elemental compositions of my samples.

Moreover, I am grateful to Finnish winter for helping me finalize this project within the limited time frame. It was so dark and cold that I didn't feel like going outside and did nothing else but working on my thesis. Many thanks to the campus cafeteria for keeping my energy level high enough to keep me going.

Last but not least, I would like to thank my parents Natalya Sakarinen and Arkadiy Sakarinen, for giving birth to me at the first place and supporting me spiritually (at times also financially!) thorough my life.

Espoo,
May 10, 2019

Ekaterina Sakarinen

CONTENTS

1. INTRODUCTION

In the past years, cellulosic materials have drawn significant attention due to their biodegradability, biocompatibility, good availability in nature, considerably low price and ease for chemical modification. [1–3] Cellulose and its semi-synthetic derivatives have versatile uses in many industries such as veterinary foods, wood and paper, fibers and clothes, cosmetic and pharmaceutical industries as excipients.[4]

Carboxymethyl cellulose (CMC) is a water soluble cellulose derivative with carboxymethyl groups bound to the cellulose backbone. Cellulose nanofibers (CNF) are resulting from a mechanical disintegration of cellulosic pulps into individual nanofibrils by, e.g. by high pressure homogenization.[2] Both CMC and CNF can absorb an enormous amounts of water and form hydrogels that are held together by fibril entanglement, ionic interaction and hydrogen bonds. The biological inertness of CMC and CNF-based hydrogels makes them promising candidates for a wide range of biomedical applications.

By chemical modification of CMC or CNF, new functionalities can be incorporated into the materials to make a value-added product. A functionality of special interest in biomedical applications is thermal response. Grafting of thermo-responsive polymer chains on CMC or CNF may introduce the desired thermo-responsive functionality to the hydrogels which would make them attractive to use in drug delivery and tissue engineering.[5–7]

In this work, the possibility of obtaining thermo-responsive cellulose hydrogels by grafting low-molecular-weight polymer chains was investigated. The polymer chains to be grafted were poly(*N*-isopropylacrylamide) (PNIPAM) and poly(di(ethylene glycol) methyl ether methacrylate) (PDEGMA); both exhibiting rapid and reversible phase transition around human body temperature.[1,8] PNIPAM and PDEGMA were first synthesized via atom transfer radical polymerization (ATRP) and then grafted onto CMC and CNF by targeting their carboxyl groups via click chemistry and amidation reactions. The thermal response of the graft copolymers was studied with UV-VIS, DLS and rheological tests.

2. THEORETICAL BACKGROUND

2.1. Cellulose and its modification

2.1.1. Cellulose

Cellulose is a fibrous and water-insoluble polysaccharide that is found in the protective cell walls of plants, particularly in stalk, stems, trunks and all woody portions of plant tissues.[9] The basic chemical structure of cellulose is presented in Figure 1. Cellulose is a linear polymer with a molecular repeat unit comprised of a pair of D-anhydroglucose ring units joined by β-1,4-glycosidic oxygen linkages around which the molecular chain can bend and twist. Each anhydroglucose unit (AGU) bears three hydroxyl groups which are mainly responsible for the chemistry reactions of native cellulose.[10] The chemistry of hydroxyl groups is similar to the one of alcohols: upon reaction, cellulose forms many of the common derivatives of alcohols, such as esters and ethers.[11]

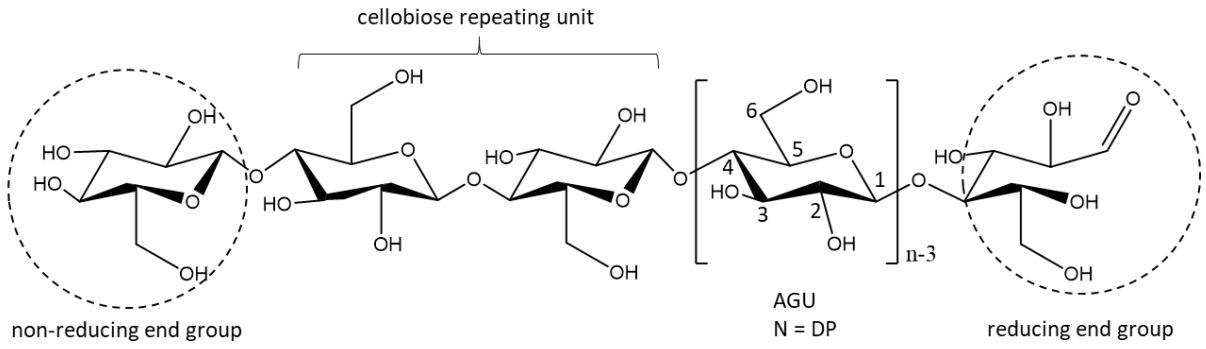

Figure 1. Chemical structure of cellulose, consisting of anhydrous glucose units (AGU), with the frequency *n*, defining the degree of polymerization (DP). Adapted from [12].

2.1.2. Cellulose nanofibers

Nanocellulose is a class of natural, sustainable materials derived from cellulose. Nanocelluloses exhibit impressive mechanical properties and tunable surface chemistries.[13] Their high surface area-to-volume ratio enables enhanced interactions with, and binding to, polymers, other nanoparticles, and small molecules. Based on their dimensions, functions, and

preparation method, nanocelluloses have been classified into three main categories (Table 1): bacterial nanocellulose (BNC), cellulose nanocrystals (CNC), and cellulose nanofibers (CNF).

Table 1. The family of nanocelluloses. Adapted from [14].

Type of nanocellulose	**Selected synonyms**	**Typical sources**	**Formation and average size**
Cellulose nanofibers (CNF)	(micro- / nano-) fibrillated cellulose; cellulose microfibrils	Wood, Sugar Beet, Potato Tuber, Hemp, Flax	Delamination of wood pulp by mechanical pressure before and/or after chemical or enzymatic treatment Width: 5 – 70 nm Length: several µm
Cellulose nanocrystals (CNC)	cellulose crystallites; (nano)whiskers; rod-like cellulose	Wood, Cotton, Hemp, Flax, Wheat Straw, Mulberry Bark, Ramie, Avicel, Tunicin, Cellulose from algae and bacteria	Acid hydrolysis of cellulose from many sources Diameter: 5 – 70 nm Length: • 100 – 250 nm (from plant sources) • 100 nm to several µm (from cellulose of tunicates, algae, bacteria)
Bacterial nanocellulose (BNC)	bacterial / microbial cellulose; biocellulose	Low-molecular-weight sugars and alcohols	Bacterial synthesis Diameter: 20 – 100 nm; different types of nanofiber networks

Cellulose nanofibers (CNF) are typically made from wood-derived fibers that have been defibrillated to the level of several hundreds of a micron and smaller as shown in Figure 2. The nanosized fibers can be extracted from any cellulose containing source, i.e. pulp. In order to extract and individualize the nanofibers from the cell walls, it is necessary to expose the pulp to high shear forces.[9] This can be done through high pressure, high temperature and high velocity impact homogenization, grinding or microfluidization.[15]

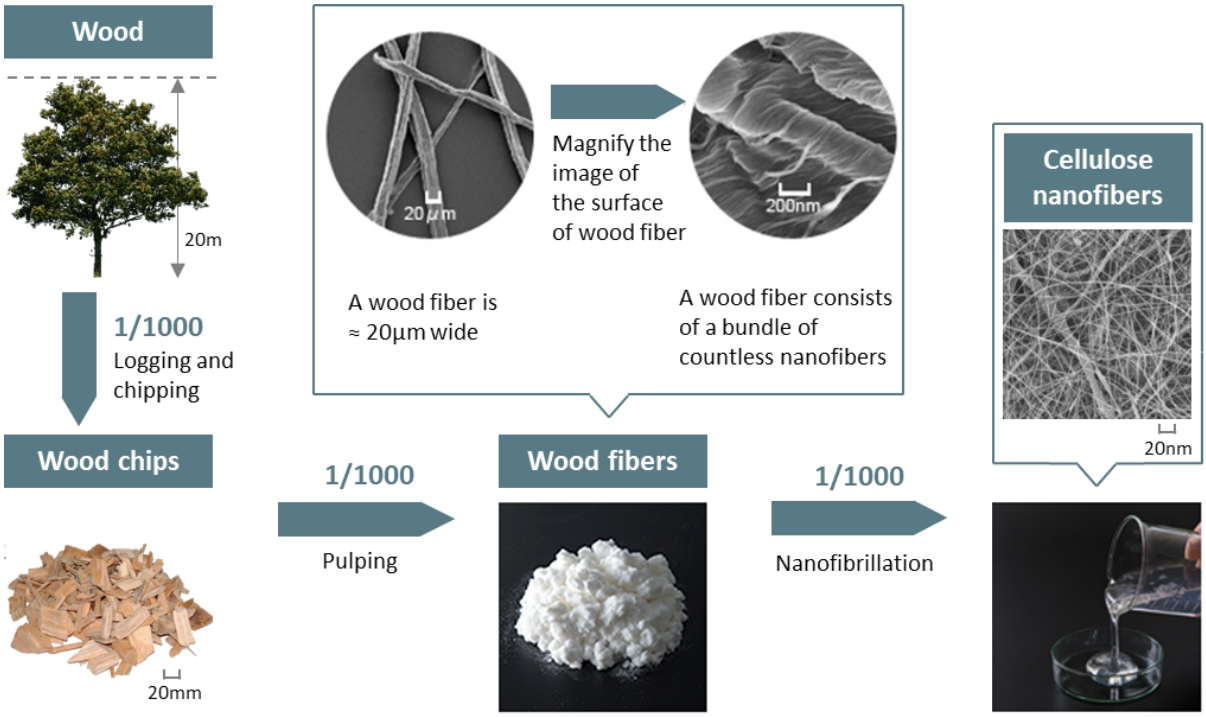

Figure 2. Wood hierarchical structure: from tree to cellulose and nanocellulose. Adapted from [16].

Turbak et al. (1983) reported the production of CNF by passing water suspension of refined wood pulp through homogenizer. Before the homogenization, cellulose was refined with PFI mill up to 10000 revolutions and passed through a homogenizer at a pressure of 8000 psi with water cooling to stabilize stable temperature of stable 70-80 ˚C.[17] Then, the cellulose slurry was fed through a spring-loaded valve assembly which opened and closed rapidly subjecting the fibers to large pressure drops with shear and impact forces, which ensured cellulose fibrillation.

Zimmermann et al. (2004) reported the use of microfluidizer for cellulose fibrillation. Sulphite pulp suspensions were passed through microfluidizer at a pressure of 1000 bar for 60 min.[18] When cellulose is passed through thin chamber of microfluidizer very high velocities are achieved with strong shear forces and impacts against channel walls. It was also reported that the CNF was produced by 5 passes of cellulose suspension through the chamber of 100 μm at a pressure of 2200 bar.[19]

Cellulose nanofibers in plant cell walls are tightly bound to one another by multiple hydrogen bonds, thus the delamination/fibrillation of cellulose fibers consumes very large amounts of energy which often presents a challenge for the industrial manufacturing. To address this

problem, the process is often combined with enzymatic treatment[20], TEMPO (2,2,6,6-tetramethylpiperidin-1-yl)oxyl) oxidation[15], or other chemical modifications (e.g., carboxymethylation[21]).

TEMPO-mediated oxidation of native cellulosic fibers is the most commonly used pretreatment to prepare CNF.[22,23] The catalytic oxidation involves a selective conversion of the primary hydroxyl (-OH) groups of the anhydroglucose units (AGUs) in the cellulose to carboxylate ($-COO^-Na^+$) groups under aqueous and mild conditions.[22–25] TEMPO-oxidized CNFs (TOCNs) have many advantages compared with other CNFs. TOCNs are characterized by their transparency, high aspect ratios (typically in a range between 100 and 1000[26]), uniform widths, and complete nano-dispersion.[23] Their surface chemistry is especially of interest, because both hydroxyl and carboxyl groups are available for chemical modification to produce value-added materials.[27]

2.1.3. Chemical modification of cellulose

Polysaccharides are widely chemically modified in order to introduce properties required for specific applications. Desired surface functionalities can be introduced to CNF and CMC by targeting their carboxylate and hydroxyl groups.

Esterification and etherification reactions are the most common, well established and optimized approaches for the chemical modification of cellulose.[27] They target the hydroxyl groups available within the AGUs of cellulose. Common, commercially produced esters and ethers from cellulose are shown in Figure 3.

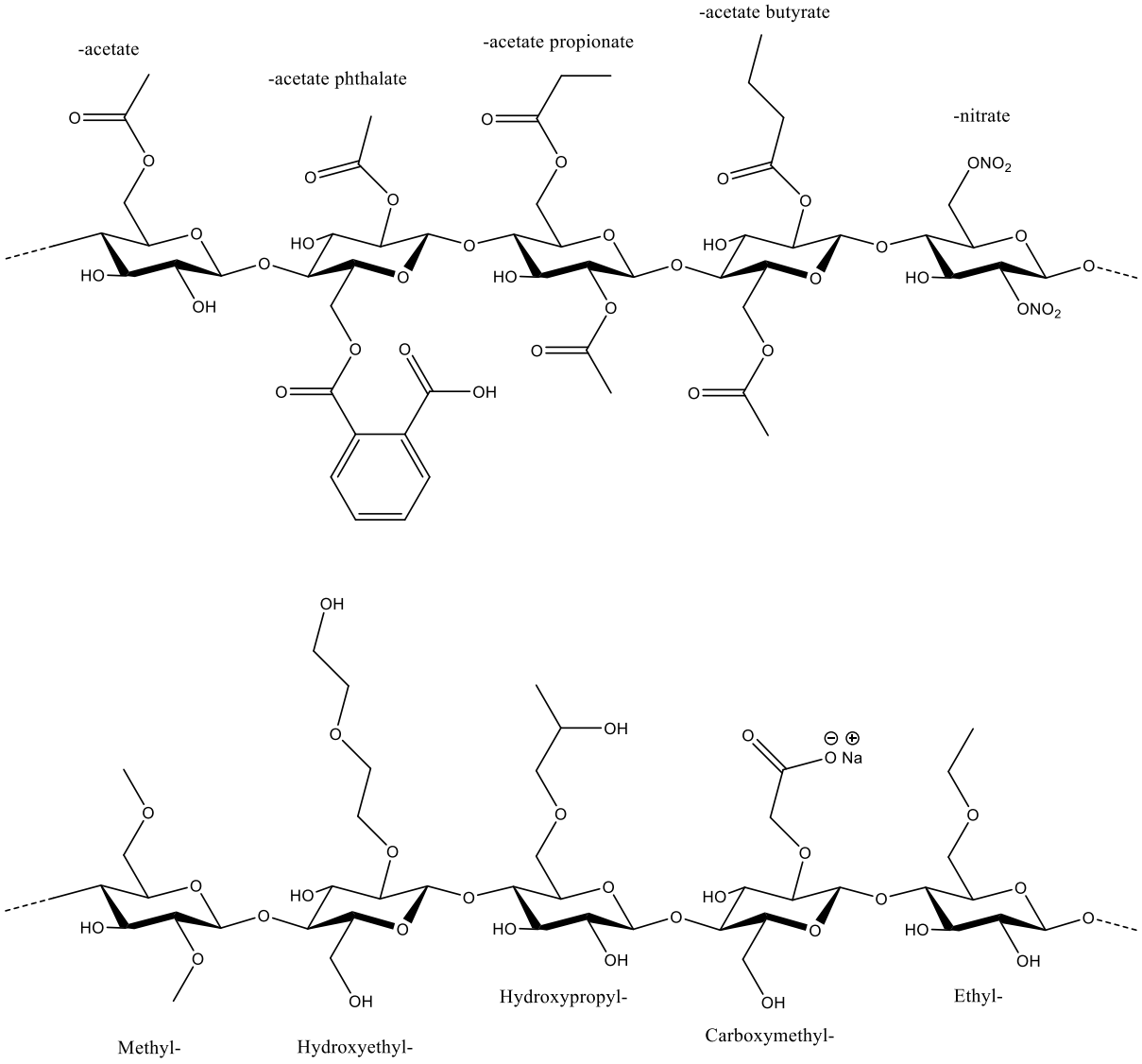

Figure 3. Schematic presentation of commercially produced cellulose esters (top) and ethers (bottom). Adapted from [27].

Sodium carboxymethyl cellulose (CMC) is a water-soluble cellulose derivative used as a thickener, phase-emulsion stabilizer, and/or suspension agent in many industries, such as food, pharmaceuticals, paints, leather, paper and oil well drilling.[8] CMC is synthesized by the alkali-catalyzed reaction of cellulose with chloroacetic acid.[28] The reaction results in binding carboxymethyl groups to some of the hydroxyl groups along the cellulose chain (Figure 1b).[28] The polar carboxyl groups render cellulose soluble and chemically reactive. The number of hydrogens in hydroxyl groups of AGU replaced by carboxymethyl groups is defined as degree of substitution (DS).[28] If all three hydroxyl groups are replaced with carboxymethyl ones, the DS is defined as 3. In practice, the DS usually lies in the range 0.6 to 0.95 and CMC is generally

considered water-soluble down to DS 0.3.[28] The functional properties of CMC, such as viscosity and solubility in water, depend mainly on the DS and also the molecular weight (MW) of the polymer.[12]

2.1.4. EDC/NHS-assisted coupling reactions

Two molecules can be covalently attached to each other by forming a bond containing no additional atoms with a help of zero-length cross-linkers. Carbodiimides are the most common cross-linkers, since they are soluble in water as well as most macromolecules of biological origin. The byproduct of the reaction, a water soluble isourea derivative, can be removed easily by dialysis or gel filtration.[29]

The most popular crosslinking agent for conjugating substances containing carboxylic groups is 1-ethyl-3-(3-dimethylaminopropyl)carbodiimide hydrochloride (EDC).[29] One of the bonds, formation of which can be mediated with EDC, is an amide linkage made by the condensation of a primary amine with a carboxylic acid.[29] EDC reacts with a carboxylate group under formation of an *O*-acylisourea leaving group which is however slow to react with amines and can hydrolyze in water. If the amine does not find the active carboxylate before hydrolysis, the desired coupling cannot occur. To address this problem, EDC is often applied together with *N*-hydroxysulfosuccinimide (NHS)[30]. This leads to an increase in stability of the active intermediate giving it more time to react with the attacking amine. EDC/NHS coupled reactions give significantly higher yields of conjugations than those obtainable solely with EDC[29]. The EDC/NHS crosslinking reaction is schematically illustrated in Figure 4.

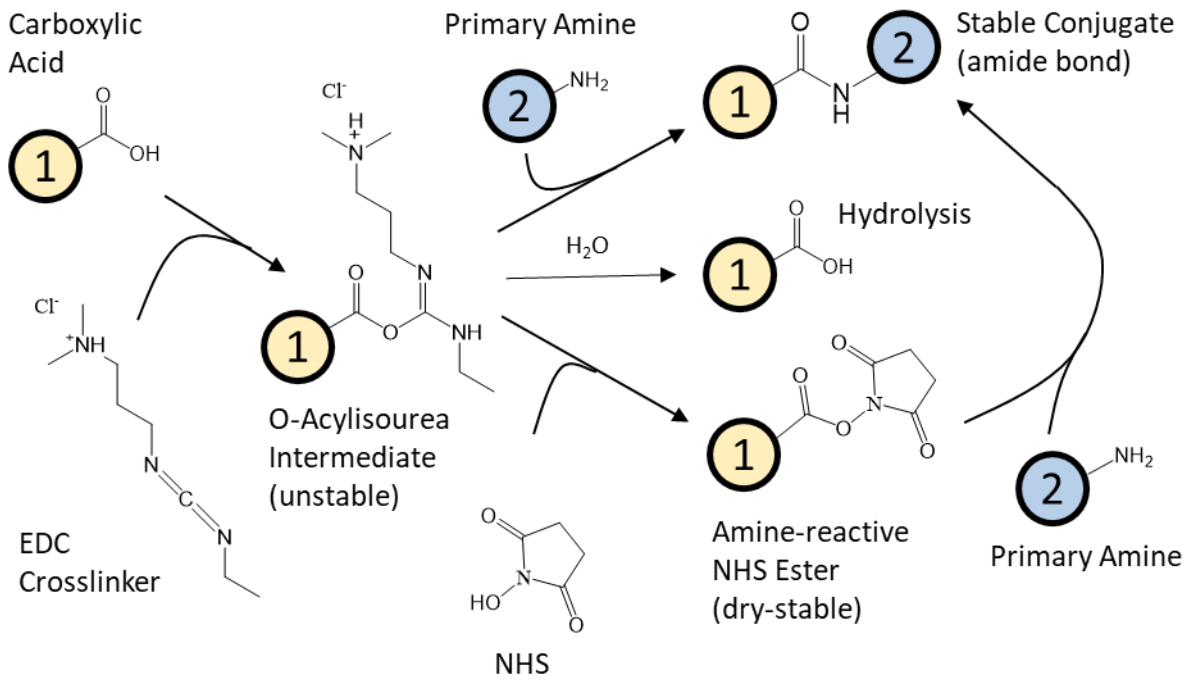

Figure 4. EDC–NHS chemistry: EDC reacts with a carboxylic-acid group on the surface of substance 1, forming an amine-reactive O-acyl isourea intermediate. This intermediate may react with an amine on substance 2, yielding a conjugate of the two molecules joined by a stable amide bond. The addition of NHS stabilizes the amine-reactive intermediate by converting it to an amine-reactive NHS ester, thus increasing the efficiency of EDC-mediated coupling reactions. Adapted from [31].

A thorough literature research on EDC/NHS-assisted grafting of thermo-responsive polymers on the surface of nanocellulose yielded only one related article. In January 2019, Gicquel et al. published a paper on grafting amine-terminated PNIPAM onto the surface of TEMPO-oxidized CNC using EDC as cross-linker. To the best of found knowledge, EDC/NHS-mediated coupling has never been employed to graft thermo-responsive polymers on CNF. However, thermo-responsive polymers were grafted with EDC/NHS chemistry onto alginate/chitosan polyelectrolyte complex[32], hydrogels composed of chitosan and hyaluronic acid[33], and CMC[34].

2.1.5. Click chemistry

Recently, Sharpless et al. (2001) introduced the term “click chemistry” to describe reactions that need no protection from oxygen, are high in yield, wide in scope and simple to perform, create only byproducts that can be removed without chromatography, and can be conducted in easily removable or mild solvents.[35] The Cu-catalyzed azide/alkyne cycloaddition (CuAAC)

has rapidly become the most popular click reaction to date.[36] CuAAC reaction tolerates aqueous conditions and can be carried out in a broad temperature and pH range (pH 4-12).[26] Copper catalysts are troublesome in biological applications but they can be removed via dialysis in low concentrated acetic acid and extraction with isobutyl alcohol.[37]

Figure 5 presents the proposed mechanism of CuAAC reaction. Molecules containing terminal alkyne and azido groups react via cycloaddition to form a triazole structure. Typically, copper sulfate and sodium ascorbate are added in a reaction to form the active Cu(I) catalyst (sodium ascorbate reduces the Cu(II) ions to Cu(I) species.[14] Furthermore, the addition of a slight excess of sodium ascorbate is often used to avoid the formation of oxidative homocoupling products.[14] Disproportionation of a Cu(II) salt in the presence of a Cu wire can also be used to form the active Cu(I) catalyst.[14]

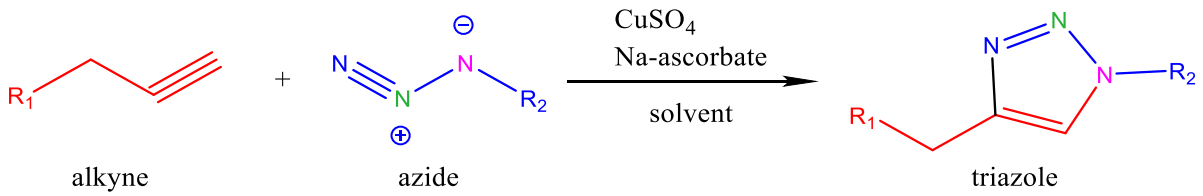

Figure 5. Mechanism of copper-catalyzed azide-alkyne cycloaddition (CuAAC) reaction. A terminal alkyne in the presence of Cu will react with an azide to form a stable triazole product.

The preparation of graft copolymers from cellulose or cellulose derivatives has been widely investigated. However, click chemistry approaches have so far been scarcely reported for the preparation of cellulose-based graft copolymers.[37] There are a few publications using click chemistry in CNF modifications [38], but grafting polymer chains onto nanocellulose still remains unstudied. Click chemistry has already been utilized to chemically bind thermo-responsive polymers with chitosan[37,39–41], native cellulose[42] and hydroxyehyl cellulose[43]. To the best of the author's knowledge, thermo-responsive polymers have never been grafted via CuAAC onto nanocellulose or CMC.

2.2. Cellulose-based hydrogels

2.2.1. Physical gels and covalently linked gels

Hydrogels are commonly defined as three-dimensional networks of polymers capable of absorbing up to thousands times their own dry weight in water.[44] They are typically classified in two categories by the nature of their reticulation points: covalently linked gels and physical gels. The former, as the name suggests, are based on polymer chains that are linked together through covalent bonds at points that are called cross-links. The latter are formed by the physical entanglement of polymer chains in solution. Temporary cross-linking is induced through several noncovalent interactions, such as ionic interaction, hydrophobic interaction, hydrogen bonding, or host-guest and stereo complexation.[30] Both of the gels, crosslinked or physical, have the ability to swell in water. However, when a physical gel is given enough time and space it will fully dissolve in water, whereas a chemically cross-linked gel will not.

2.2.2. Thermo-responsive hydrogels

Thermo-responsive hydrogels find a variety of biomedical applications, such as drug delivery, gene delivery, wound healing, and tissue engineering. Figure 6 illustrates how hydrogel systems can be used as drug or gene delivery systems or tissue regeneration matrices. Firstly, drugs, genes, and/or cells are mixed with the low-viscous polymer solution at room temperature. Secondly, the modified polymer solution is injected directly to the defect area through a syringe. Then polymer solutions exhibit physical or chemical cross-linking in response to the temperature change triggering the gelation inside the body. In contrast with chemically crosslinked networks, physical hydrogels are beneficial for sustained delivery applications since they are easy to inject with a syringe, more prone to disintegrate in the body, and avoid use of toxic cross-linkers.[30]

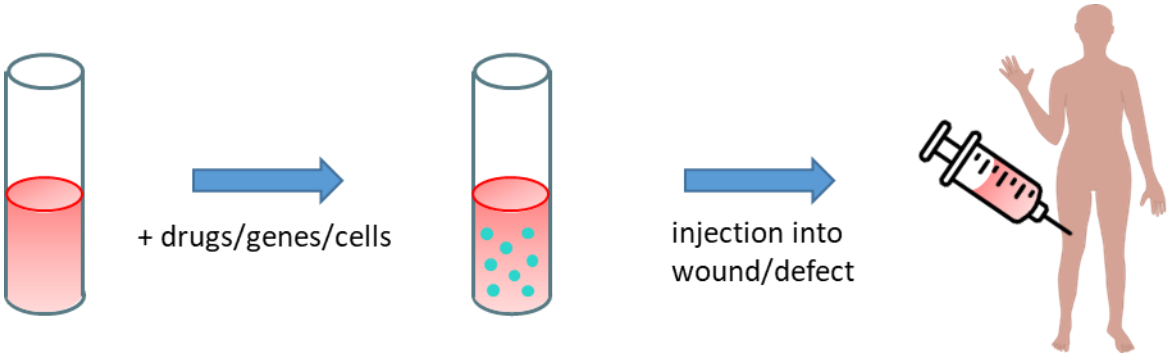

Figure 6. Injectable drug/gene delivery systems and tissue regeneration matrices. Drugs, genes or cells are dispersed in the polymer solution and then injected to form *in situ* hydrogels via physical and/or chemical crosslinking.

In tissue engineering, thermo-responsive hydrogels can be used to encapsulate cells in 3D structures in the body. Such hydrogels allow for the delivery of encapsulated cells, nutrients and growth factors to defects of any shape using minimally invasive techniques. The basic idea of the in-situ formation of cell/scaffold is shown in Figure 7.

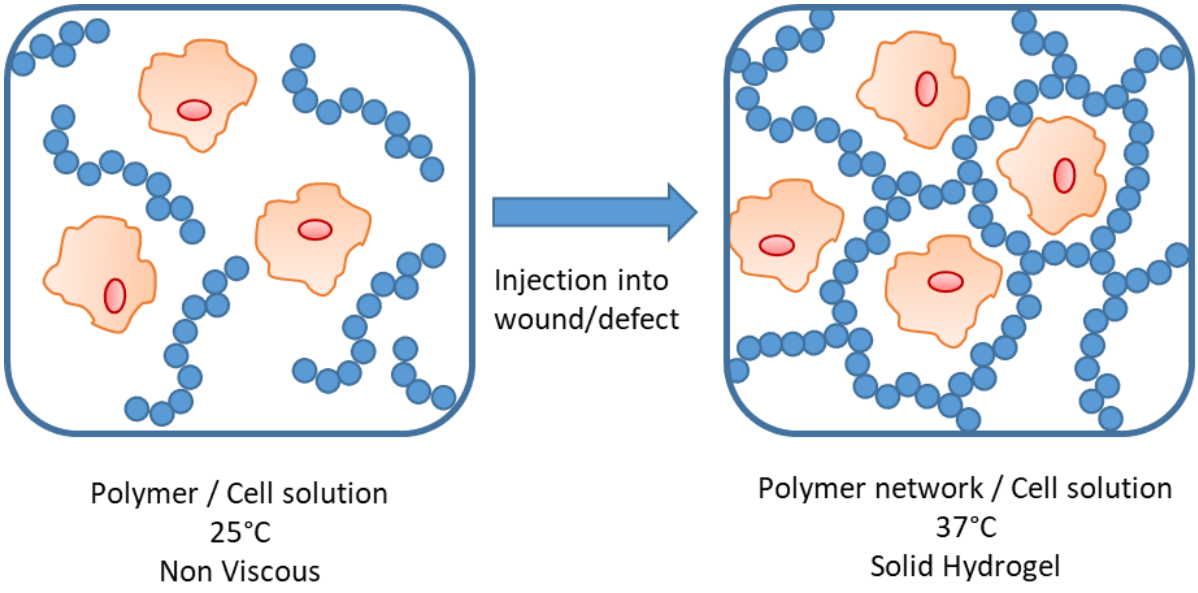

Figure 7. *In-situ* formation of a scaffold in tissue engineering. Thermo-responsive polymer is mixed at room temperature with cells and then injected into the body. Upon injection due to the temperature increase the polymer forms a physical gel. The cells are encapsulated within the 3D structure of the gel.

2.3. Cellulose-based graft copolymers

In this study, CMC and CNF were attempted to be modified with thermo-responsive polymers in order to introduce thermal response to the cellulose based hydrogels. Low-molecular-weight polymer chains were used to overcome the limitation of the celluloses accessibility.

2.3.1. Thermo-responsive polymers

Thermo-responsive polymers can be classified in two categories: those that become insoluble above a critical temperature called the lower critical solution temperature (LCST) as shown in Figure 8, and those that precipitate and undergo phase change below a critical temperature called the upper critical solution temperature (UCST).[45] In general, most of the polymers studied in biomedical applications exhibit LCST, since they display ideal phase transition between room and body temperature.[30] They are attractive since they are soluble at low temperature and form a viscoelastic gel after subcutaneous injection into warm-blooded animals and humans. The phase transition of such polymers is present due to inter- and intramolecular hydrogen bonds between water molecules and the polymer chains.[46] LCST depends on polymer degree of polymerization and branching as well as the polymer's composition and architecture.[47]

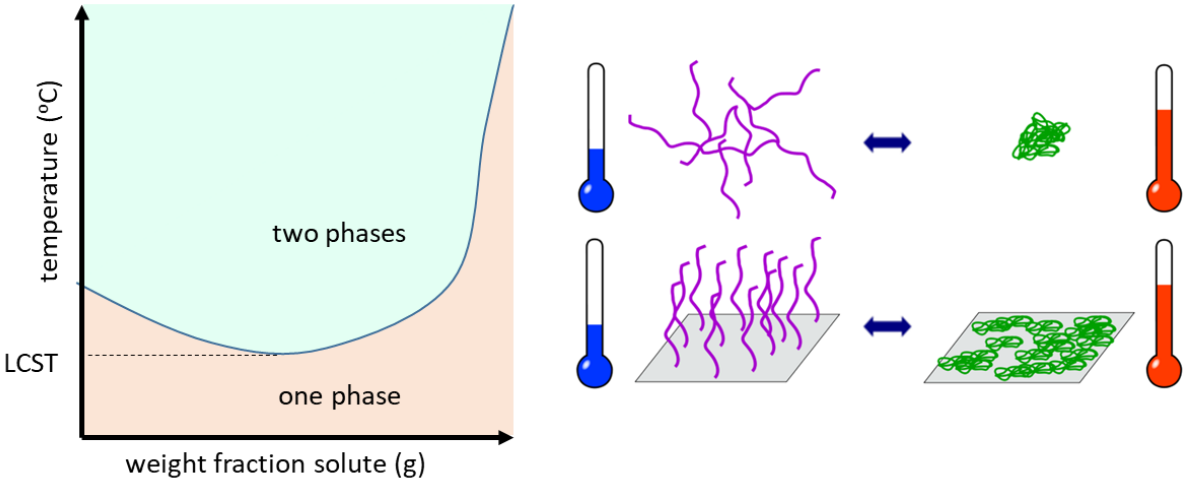

Figure 8. Typical Phase diagram of a system exhibiting lower critical solution temperature (LCST). Below LCST, the polymer chains are in form of hydrophilic coils and above LCST they exhibit sol-gel transition to hydrophobic globules.

The most studied thermo-responsive polymer is poly(*N*-isopropylacrylamide) (PNIPAM). [34] The chemical structure of PNIPAM is shown in Figure 9. The LCST of PNIPAM has been reported to be in a range of 30-36 °C, but most frequently it is assigned to a value of 32 °C, which garnered considerable attention since it is near human body temperature.[24,48] At low temperatures, the polymer is soluble in water due to the hydrogen bonding between hydrophilic amine groups and water molecules.[34] As the temperature of polymer solution approaches the transition point, hydrophobic interactions among isopropyl groups become stronger, while the polymer-solvent hydrogen bonds become weaker, leading to the collapse of the polymer molecules and the formation of hydrophobic globules.[34] The LCST of PNIPAM water solutions is slightly dependent on the concentration but most importantly on the MW of the polymer; i.e. 5000 g/mol PNIPAM shows a LCST of 38 °C, whereas 8000 g/mol PNIPAM shows a LCST of 36 °C and 12000 g/mol PNIPAM shows LCST of 34 °C. Recently published results by Vihola et al. (2005) propose that acrylamide-based polymers show cytotoxicity at the physiological temperature[49]; therefore, nontoxic thermo-responsive polymer alternatives are being explored.

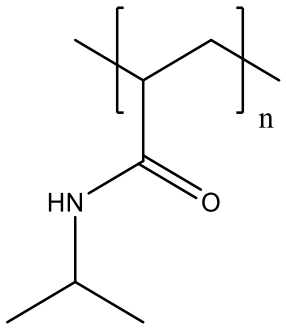

Figure 9. Chemical structure of poly(*N*-isopropylacrylamide) (PNIPAM).

Another promising group of thermo-responsive polymers is poly(ethylene glycol) methacrylates (PEGMAs), which have shown to be nontoxic and biocompatible.[1,50] Figure 10 shows the family structure of ethylene glycol methacrylates (EGMAs). EGMAs consist of a methacrylate part and an ethylene glycol part. The difference between the members of the family is the number of ethylene glycol segments in the side-chain. The ethylene glycol part makes the polymer hydrophilic, because of hydrogen bonding to water caused by oxygen atoms. Hence, the longer the ethylene glycol chain, the more hydrophilic the resulting polymer is.[1] However, EGMAs are still hydrophobic above certain temperature (LCST) due to the

presence of the methacrylate part. The LCST of these polymers can be tuned in the range of 26-90 °C by changing the length of the ethylene glycol segment in the side chain.[1] The more ethylene glycol groups, the higher is the LCST of the substance. For instance, poly(di(ethylene glycol) methyl ether methacrylate) $PMEO_2MA$, also named PDEGMA, (2 ethylene glycol groups) has a LCST of around 27 °C[51], whilst poly(oligo(ethylene glycol) methyl ether methacrylate) POEGMA (4-5 ethylene glycol groups) has a LCST of 73 °C[1].

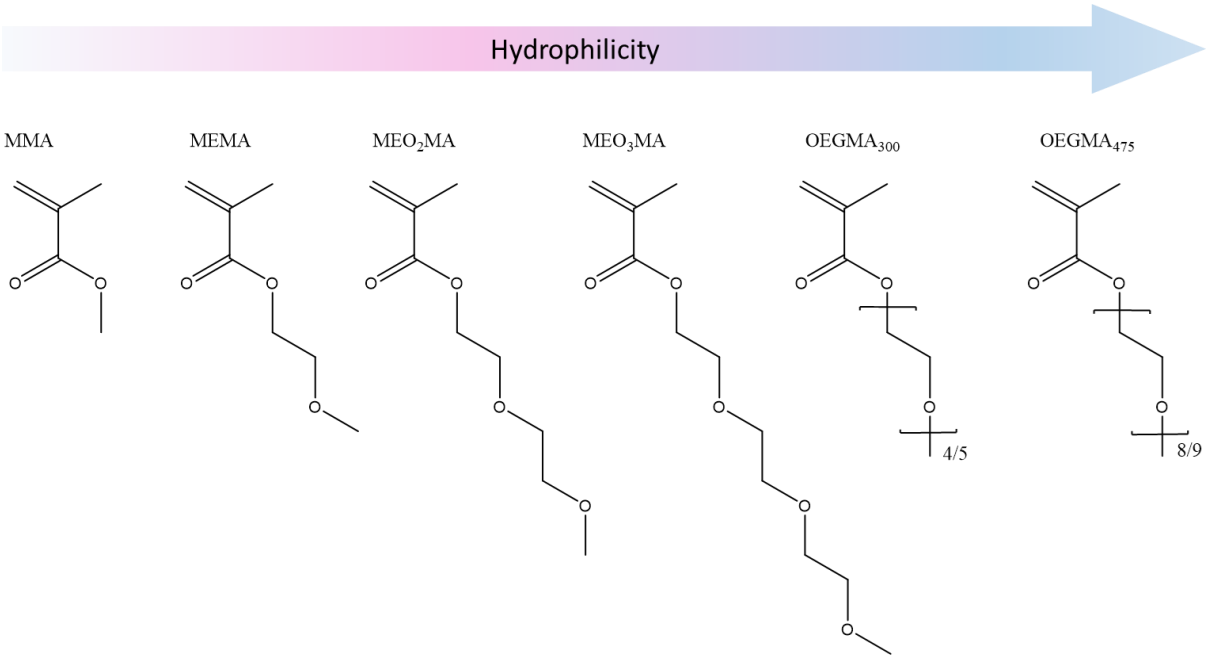

Figure 10. Family of ethylene glycol methacrylates (EGMAs) Adapted from [51].

2.3.2. "Grafting to" and "grafting from" cellulosic substrates

Thermo-responsive polymers can be covalently bound to cellulosic substrates with two different approaches, namely "grafting to" (i.e. to the surface) and "grafting from". In the "grafting from" method, polymerization occurs directly from the surface. The surface is first functionalized with an initiator monolayer. Then, the polymerization is carried out on the initiated surface.[52] This approach yields high grafted layer densities but often uses toxic solvents or reagents and the characterization of grafted chains is a great challenge. In the "grafting to" method, a pre-synthesized end-functionalized polymer is coupled with a reactive surface. This approach generates deposited layers with lower densities and limited thickness

due to the steric hindrance during grafting and diffusion processes.[53] However, the grafted polymer can be well characterized prior to the reaction.[37]

In this work, the "grafting to" synthetic route is utilized due to the higher purity and more defined structure of the grafted polymer chains. This also allowed to avoid using aggressive solvents which are a limitation for biomedical applications.[53] Polymers were synthesized via atom transfer radical polymerization (ATRP) prior to their attachment.

2.3.3. Atom transfer radical polymerization (ATRP)

Atom transfer radical polymerization (ATRP) is one of the most efficient controlled radical polymerizations. It has attracted commercial interest because of its easy experimental set-up, use of readily accessible and inexpensive catalytic components and simple initiators.[54] ATRP is a simple route to obtain well-defined polymers with predetermined molecular weight, narrow molecular weight distribution and preselected chain end functionality.[7,55] These polymers can be prepared over a range of temperatures and without formation of side products.

However, there are several drawbacks of using ATRP to synthesize polymers. To start with, conventional ATRP is fairly sensitive to oxygen. Small amounts of oxygen will be scavenged by the catalyst and will not completely prevent the polymerization from proceeding. However, oxidation of the catalyst will reduce the catalyst´s concentration and thus slow down the reaction. [54] Another disadvantage of the ATRP method is the required use of large amounts of the CuX/ligand catalyst complex. Removal and recycling of the catalyst is one of the main challenges for the commercialization of the process. The extra purification step is associated with longer time needed to obtain the final product, and generates chemical waste.[56]

ATRP is a complex process based on several elementary reactions: initiation, propagation, and termination. The scheme in Figure 11 summarizes a typical ATRP reaction. The radicals, or the active species are generated through a reversible redox process catalyzed by a transition metal complex (Mt^n/L) which undergoes a one-electron oxidation with abstraction of a halogen atom, X, to form a dormant species, P_n-X. This process occurs with a rate of constant of activation k_{act}, and deactivation k_{deact}. Polymer chains grow by addition of the intermediate radicals to monomers with the rate constant of propagation k_p. Termination (k_t) occurs mainly

through combination or disproportionation and is the most significant at the beginning of the polymerization.[54]

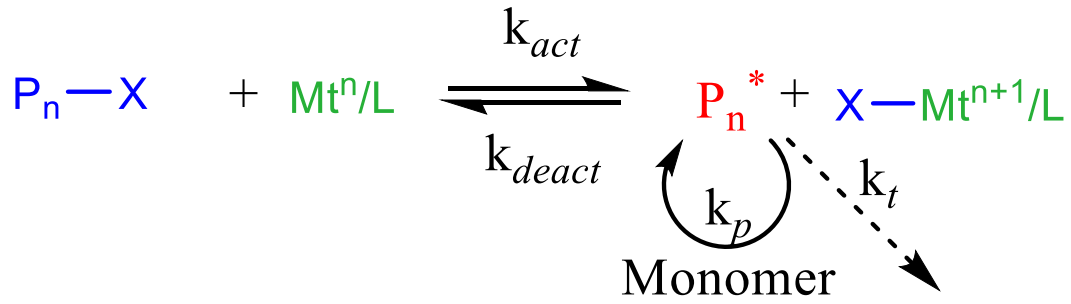

Figure 11. General scheme for an ATRP reaction [57], where Pn-X is a dormant species (X = Br, Cl), Mtn/L is a metal catalyst/ligand complex, Pn* is a propagating radical, Mtn+1/L is a metal catalyst in a higher oxidation state, kact and kdeact are activation and deactivation rate constants, respectively, kp is a propagation rate constant and kt is a termination rate constant.

If initiation is fast and termination and transfer are negligible, then the number of growing chains is constant and equal to the initial initiator concentration.[54] Hence, the theoretical number-average molecular weight (M_n) of polymers prepared by ATRP may be calculated as follows:

$$M_n = ([M]_0 / [\text{initiator}]_0) \times \text{conversion} \times M_W(M) \quad (1)$$

where $[M]_0$ and $[initiator]_0$ are the initial concentrations of monomer and initiator in the feed and $M_W(M)$ is the molecular weight of the monomer unit. Since the initial concentrations of reagents in the feed and the molecular weight of the monomer unit are constants, the M_n of the ATRP polymers increases linearly with increasing conversion.

3. MATERIALS & METHODS

3.1. Materials

Sodium carboxymethyl cellulose (CMC, Mw ~ 250000, DS 0.7), *N*-isopropylacrylamide (NIPAM, 97 %), *N*-(3-(dimethylamino)propyl)-N'-ethylcarbodiimide hydrochloride (EDC), *N*-hydroxysuccinimide (NHS, 98 %), copper (I) bromide (CuBr, 99.999 %), 1,1,4,7,10,10-hexamethyltriethylenetetramine (HMTETA, 97%), ethyl 2-chloropropionate (ECP, 97 %), di(ethylene glycol) methyl ether methacrylate (DEGMA, 95 %), amine-terminated poly(NIPAM) (PNIPAM-NH_2, M_n 2500), azide-terminated poly(NIPAM) (PNIPAM-N_3, M_n 5000), activated neutral alumina, sodium azide (NaN_3, 99.5 %), propargylamine hydrochloride (propargyl-NH_2, 95 %), α-bromoisobutyryl bromide (BIBB, 98 %), tris(2-dimethylaminoethyl)amine (Me_6TREN, 97 %), copper (I) chloride (CuCl, 99.995 %), dimethylformamide (DMF, 99.8 %), α-bromoisobutyryl bromide (BIBB, 98 %), *N*-Boc-ethylenediamine (BOC-NH_2, ≥ 98 %), trimethylamine (for synthesis), copper (II) sulfate pentahydrate ($CuSO_4 \cdot H_2O$, 99 %), sodium L-ascorbate (99 %), acetic acid (99 %) and isopropanol (IPA, 99.8 %) were purchased from Sigma Aldrich. Tetrahydrofuran (THF, 99.5 %), n-hexane (99 %), toluene (98 %), trifluoroacetic acid and chloroform-d (CD_3Cl) were purchased from VWR International Oy. Methanol (MeOH, 99.8 %) was purchased from Merck. Specra/Por tubular dialysis membranes with molecular weight cut-off (MWCO) of 1, 3.5 and 12-14 kDa were purchased from Spectrum Medical Industries.

Prior to use, monomers were purified from inhibitors that prevent polymerization. NIPAM was recrystallized from a mixture of hexane/toluene (10:1, v/v). During recrystallization, impure NIPAM was dissolved in the hot solvent mixture until the solution was saturated, and then the liquid was allowed to cool. The compound then formed relatively pure crystals. Any impurities that were present in NIPAM remained in the solution. The crystals were isolated with vacuum filtration and vacuum dried. DEGMA was purified by passing through a column filled with activated neutral alumina. The column was filled with circa 10 cm dry alumina and wetted with MeOH. Then a mixture of DEGMA/MeOH (1:1, v/v) was dripped through and the solvent was removed via rotary evaporation. CNF was prepared via TEMPO mediated oxidation from dissolving pulp by Dr. Katja Heise. All the other compounds were used as received. All water used in this study was purified with a Millipore Milli-Q system.

3.2. Characterization

3.2.1. Dry matter content analysis

2-5 mL of a sample was weighed into a pre-dried vial and oven-dried at 60 °C. DMC was calculated as follows:

$$DMC\ (\%) = \frac{m_2 - m_1}{m_3 - m_1} \times 100\ \% \quad (2)$$

where m_1 was the mass of the vial, m_2 was the mass of the liquid sample, m_3 was the mass of the dry sample after 60 °C.

3.2.2. Nuclear magnetic resonance (NMR)

^{1}H-NMR spectra were recorded at room temperature on a Bruker Avance III 400 MHz spectrometer, using $CDCl_3$ as a solvent. The measurements were performed in disposable NMR tubes, and 8 scans were accumulated. All samples were prepared by dissolving a few drops of the sample in 0.7 mL $CDCl_3$.

3.2.3. Dynamic light scattering (DLS)

DLS measurements were performed on Malvern ZS ZEN3600 instrument. Samples were diluted in MilliQ water at 1 mg/mL concentration, transferred in disposable transparent plastic cuvettes and scanned from 15 to 50 °C. Modified CNF samples were measured after dialysis without drying to prevent redispersion problems and their exact concentration was unknown.

3.2.4. Ultraviolet-visible (UV-Vis) spectroscopy

Phase transitions of the (co)polymers in water were observed by optical transmittance changes using the UV-Vis spectrometer (Schimadzu model TCC-240A) equipped with a temperature-controlled cell holder. All samples were measured at a specific wavelength (500 nm) at different temperatures. The temperatures were adjusted manually. Samples were prepared as follows: 3 mg of a dry sample was dissolved in 3 mL of MilliQ water and transferred to a 1 cm path length quartz cuvette. Modified CNF samples were measured after dialysis without drying to prevent redispersion problems and their exact concentration was unknown.

3.2.5. Attenuated total reflectance infrared spectroscopy (ATRIR)

ATRIR characterization of dry samples was performed with a Perkin Elmer Spectrum 2 (FT-IR with ATR) spectrometer in transmittance mode. Spectra were acquired for a total of 64 scans in the wavenumber range from 4000 to 450 cm^{-1} with a resolution of 4 cm^{-1}.

3.2.6. Rheology

Rheological measurements of CMC and CMC-*g*-PNIPAM copolymers in water were performed on an Anton Paar PhysicaMCR 201 rheometer, equipped with a 50-mm diameter parallel plate geometry. The gap between the plates was zeroed prior to measurements at 20 °C and kept at 1 mm during the measurements. Firstly, strain sweep experiments were carried out to determine the linear viscoelastic region. Secondly, the polymer solutions were submitted to frequency sweep tests. The temperature was controlled within ± 0.1 °C using a Peltier lower plate and a Peltier hood that were connected to a Julabo F25 circulator. Sample evaporation was minimized by employing a solvent trap. Strain sweep (γ = 0.01 … 100 %) experiments were performed at an angular frequency of 100 rad/s at 20 °C. Frequency sweep (ω = 1 … 100 rad/s) experiments were carried out at a strain amplitude of 1 % ensuring linear viscoelastic response. The polymer solutions were prepared by adding the appropriate amount of CMC (4-6 wt%) or CMC-*g*-PNIPAM (6 wt%) in water, under magnetic stirring for at least 24 h before analysis.

3.3. Synthesis of amine-terminated ATRP initiator

In the first reaction step, 0.2311 g (1.05 eq.) Et_3N and 0.2439 g *N*-Boc-ethylenediamine (BOC-NH_2) were dissolved in 5 mL THF (50-mL round-bottom flask) on ice and under continuous stirring. To the solution, 0.5 g (1 eq.) α-bromoisobutyryl bromide (BIBB) in 1 mL THF were introduced dropwise (syringe) with another 1 mL of solvent and the reaction mixture was further cooled on ice. After complete addition of BIBB, the reaction flask was purged with nitrogen for 10 minutes. Then, the ice bath was removed and the mixture was stirred for 48 hours at room temperature (RT). The Boc-protected intermediate was isolated by removing the salt precipitate over a glass fiber filter (G4), followed transferring the supernatant into a 100-mL round-bottom flask and reducing it in vacuo. The Boc-deprotection was carried out

with trifluoroacetic acid (TFA) after dissolving the solid residue in 3 mL DCM and dropwise addition of 1.5 mL TFA (syringe) on an ice bath, followed by stirring the mixture for 24 hours at RT. After the reaction, the excess of TFA and solvent were removed in vacuo (repeated addition of DCM for complete removal of TFA), followed by dissolving the solid residue in 5 mL Milli-Q water and extraction with DCM (extraction funnel). The water fraction was collected and the purified *NH_2*-terminated ATRP initiator was finally obtained after removing the water in vacuo and lyophilization.

3.4. Synthesis of amine-terminated PDEGMA (PDEGMA-*NH_2*)

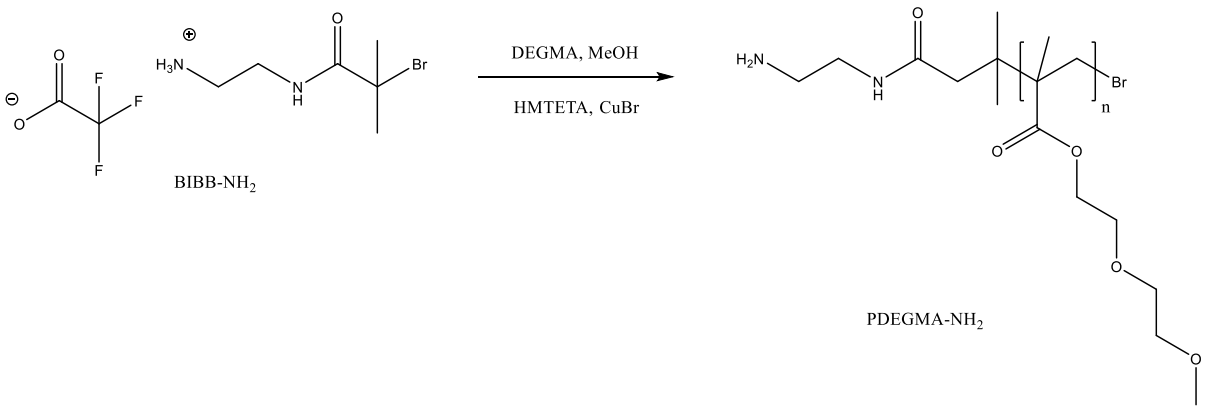

Figure 12. Synthetic route for preparation of PDEGMA-*NH_2*.

PDEGMA was synthesized by means of ATRP with BIBB-*NH_2*/CuBr/HMTETA as the initiator/catalyst/ligand system. In a general procedure, CuBr (0.0305 g; 0.21 mmol), HMTETA (0.0979 g; 0.43 mmol) and DEGMA (4 g; 21.25 mmol) were dissolved in 3 mL MeOH and degassed by purging with nitrogen. BIBB-*NH_2* (0.0686 g; 0.21 mmol) was dissolved in 0.9 ml MeOH, degassed separately, and quickly transferred to the reaction mixture with a nitrogen-purged syringe. The polymerization reaction was then initiated by placing the flask in oil preheated to 60 °C. The reaction was allowed to proceed under magnetic stirring at 60 °C for 1-4 h. To monitor the polymerization kinetics, samples were periodically withdrawn with a nitrogen-purged syringe and used for NMR analysis. The reaction was terminated by exposing it to air and putting the flask on ice. The reaction mixture was then diluted with THF, and the copper catalyst was removed from the mixture by passing through a neutral alumina column. After most of the THF was removed via rotary evaporation, the polymer was dissolved in a small amount of Milli-Q water and dialyzed against Milli-Q water for 3 days using a dialysis membrane with a molecular-weight-cutoff (MWCO) of 1 kDa. The dialysis water was

changed twice a day. The obtained homopolymer was then freeze-dried and denoted as PDEGMA-NH_2. **PDEGMA-NH_2 #1** and **PDEGMA-NH_2 #2** were polymerized for 60 and 73 min, respectively.

Table 2. Kinds of PDEGMAs obtained via ATRP.

Code	Reaction time (min)	Conversion (%)	Theoretical MW (g/mol)
PDEGMA-NH_2 #1	60	28	5250
PDEGMA-NH_2 #2	73	52	9770

3.5. Synthesis of CMC graft copolymers via EDC/NHS chemistry

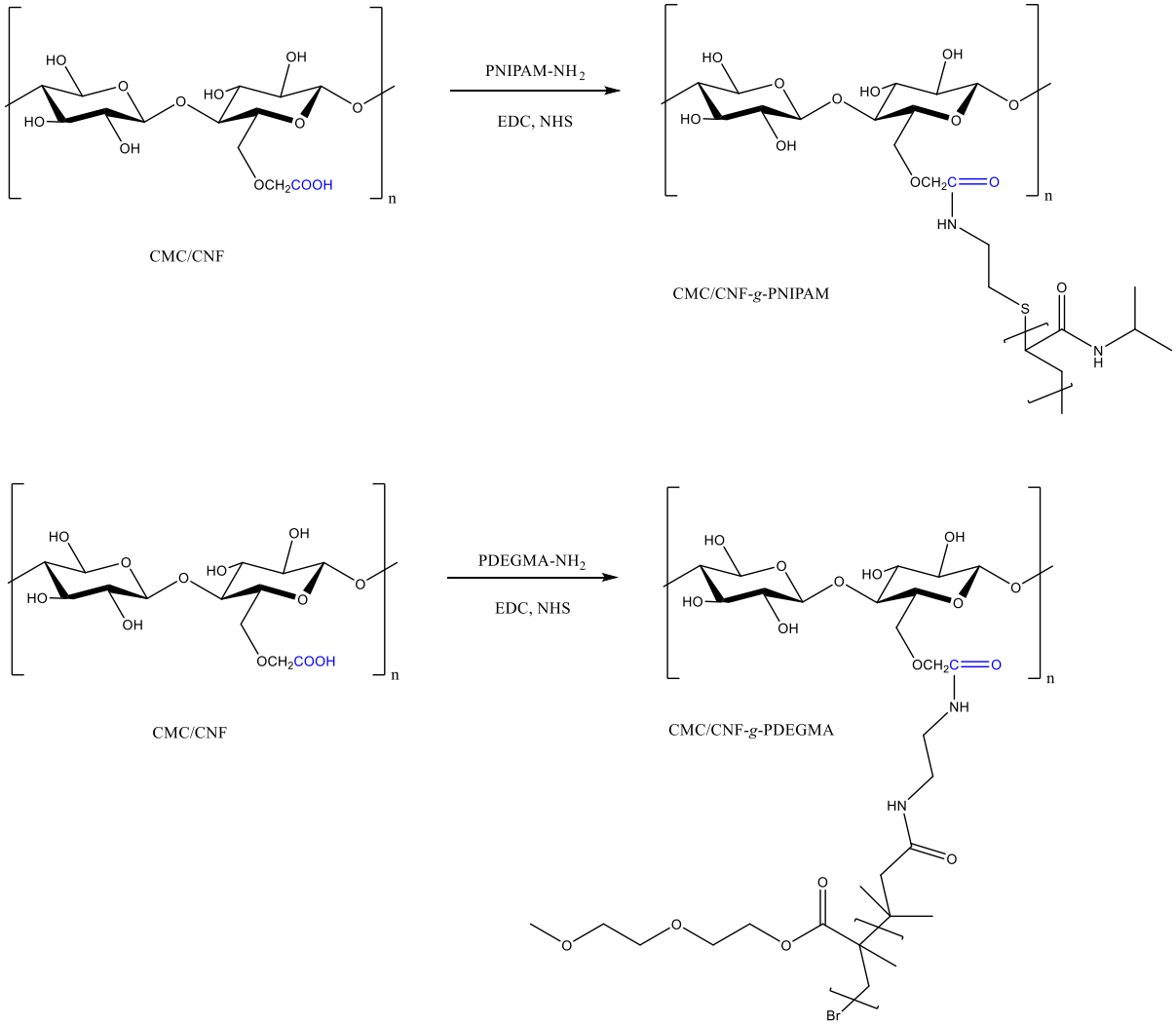

Figure 13. Synthetic route for preparation of CMC/CNF-*g*-PNIPAM and CMC/CNF-*g*-PDEGMA.

In a typical reaction of grafting polymer chains onto CMC, CMC (0.2 g; 0.92 mmol) was first allowed to dissolve in 40 ml water. NHS (0.124 g; 1.1 mmol) was added to the solution and it was stirred for 30 min at room temperature. Then, EDC (0.352 g; 1.8 mmol) was added to the solution and allowed to stir for further 90 min. Finally, polymer predissolved in 1-2 mL of water was added to the mixture and allowed to react for 48 h. The polymers grafted onto CMC were PDEGMA-NH_2 #1 and PNIPAM-NH_2 (Sigma Aldrich). The exact amounts of added polymers are listed in Table 3. No pH adjustment was carried out during the reactions. After 48 h, the reaction mixture was dialyzed against Milli-Q water for 5-7 days using a dialysis membrane with a MWCO 3.5 kDa (for PNIPAM) and 12-14 kDa (for PDEGMA). The dialysis water was changed twice a day. After dialysis, the samples were freeze-dried.

Table 3. Kinds of modified CMC obtained via EDC/NHS chemistry. *The molar amount of PDEGMA-NH_2 was estimated from the theoretical MW values.

Code	Polymer	m (polymer) (g)	n (polymer) (mmol)
CMC-*g*-PNIPAM #1	PNIPAM-NH_2 (Sigma Aldrich)	0.230	0.1
CMC-*g*-PNIPAM #2	PNIPAM-NH_2 (Sigma Aldrich)	0.691	0.28
CMC-*g*-PNIPAM #3	PNIPAM-NH_2 (Sigma Aldrich)	1.149	0.46
CMC-*g*-PDEGMA	PDEGMA-NH_2 #1	0.100	0.02*

3.6. Synthesis of CNF graft copolymers via EDC/NHS chemistry

In a typical reaction of grafting polymer chains onto CNF, 9.33 g wet CNF (0.14 g dry CNF) was first diluted with 18 mL water. NHS (0.124 g; 1,1 mmol) was added to the solution and it was stirred for 30 min at room temperature. Then, EDC (0.354 g; 1,8 mmol) was added to the solution and allowed to stir for 90 more min. Finally, polymer predissolved in 1 mL of water was added to the mixture and allowed to react for 48 h. The polymers grafted onto CNF were PDEGMA-NH_2 #2 and PNIPAM-NH_2 (Sigma Aldrich). The exact amounts of added polymers are tabulated in Table 4. No pH adjustment was carried out during the reactions. After 48 h, the reaction mixture was dialyzed against Milli-Q water for 5-7 days using a dialysis membrane with a MWCO 3.5 kDa (for PNIPAM) and 12-14 kDa (for PDEGMA). The dialysis water was changed twice a day. A part of the liquid was freeze-dried after dialysis in order to characterize it with ATRIR and determine its elemental composition. The rest of the modified CNF was not dried in order to prevent redispersion problems.

Table 4. Kinds of modified CNF obtained via EDC/NHS chemistry. *The molar amount of PDEGMA-*NH_2* was estimated from the theoretical MW values.

Code	Polymer	m (polymer) (g)	n (polymer) (mmol)
CNF-*g*-PNIPAM #1	PNIPAM-NH_2 (Sigma Aldrich)	0.116	0.05
CNF-*g*-PNIPAM #2	PNIPAM-NH_2 (Sigma Aldrich)	0.193	0.08
CNF-*g*-PNIPAM #3	PNIPAM-NH_2 (Sigma Aldrich)	0.350	0.14
CNF-*g*-PDEGMA	PDEGMA-NH_2 #2	0.19	0.019*

3.7. Adsorption studies

In order to check whether amine-terminated polymers tend to adsorb on the surface of the celluloses, CMC and CNF were mixed with PNIPAM-NH_2 in absence of the coupling agents, stirred for 48 h and purified.

CMC-*ads*-PNIPAM was prepared as follows. CMC (0.2 g: 0.92 mmol) was allowed to dissolve in 40 ml water. Then, PNIPAM-NH_2 (Sigma Aldrich, 0.691 g: 0.28 mmol) predissolved in 2 mL of water was added to the mixture and the mixture was allowed to stir for 48 h.

CNF-*ads*-PNIPAM was prepared as follows. 9.33 g wet CNF (≈0.14 g dry CNF) was first diluted with 18 ml water. Then, PNIPAM-NH_2 (Sigma Aldrich, 0.354 g: 0.14 mmol) predissolved in 1 mL of water was added to the mixture and the mixture was allowed to stir for 48 h.

In the first purification step, both CMC-*ads*-PNIPAM and CNF-*ads*-PNIPAM were dialyzed against Milli-Q for 7 days using a dialysis membrane with a MWCO 3.5 kDa and partially freeze-dried for ATR-IR analysis. In the second step, the never-dried samples were purified against Milli-Q for 7 days using a dialysis membrane with a MWCO 12-14 kDa and partially freeze-dried for ATR-IR analysis again. In the third step, the never-dried samples were first mixed with 200 mL 0.2 M KCl and allowed to stir for 2 h. Then, the mixtures were dialyzed against Milli-Q for 10 days with a 12-14 kDa MWCO membrane and freeze-dried.

3.8. Synthesis of azido-terminated PNIPAM (PNIPAM-N_3)

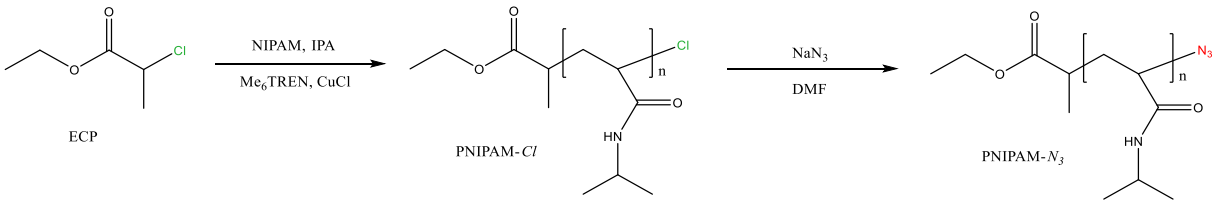

Figure 14. Synthetic route for preparation of PNIPAM-N_3.

PNIPAM was synthesized by means of ATRP with ECP/CuCl/Me_6TREN as the initiator/catalyst/ligand system. CuCl (0.05 g, 0.5 mmol), Me_6TREN (0.116 g, 0.5 mmol) and NIPAM (2.82 g, 25 mmol) were dissolved in 6.5 mL IPA and degassed by purging with nitrogen. ECP (0.064 mL, 0.5 mmol) was dissolved in 0.7 ml IPA, degassed separately, quickly transferred to the reaction mixture with a nitrogen-purged syringe, and the polymerization reaction was then initiated. The reaction was allowed to proceed under magnetic stirring at room temperature for 4 h 20 min. To monitor the polymerization kinetics, samples were periodically withdrawn with a nitrogen-purged syringe and used for NMR analysis. The reaction was terminated by exposing it to air and putting the flask on ice. The reaction mixture was then diluted with THF, and the copper catalyst was removed from the mixture by passing through a neutral alumina column. After most of the THF was removed via rotary evaporation, the polymer was dissolved in a small amount of Milli-Q water and dialyzed against Milli-Q water for 3 days using a dialysis membrane with a MWCO of 1 kDa. The dialysis water was changed twice a day. The obtained homopolymer was then freeze-dried and denoted as **PNIPAM-*Cl***. The NMR analysis revealed 77 % conversion and thus theoretical MW of the polymer was 4260 g/mol.

In order to obtain the azido-terminated PNIPAM, all PNIPAM-*Cl* (except for the tiny fraction used for NMR analysis) and NaN_3 (0.080 g, 1.21 mmol) were dissolved into 10 mL DMF in a 25-mL round-bottomed flask. The mixture was allowed to react under stirring at 45 °C (in oil) for 48 h. After removing DMF with rotary evaporation, the residue was redissolved in 50 mL of THF and passed through a neutral alumina column to remove sodium salt and excess NaN_3. The filtrate was concentrated by rotary evaporation, dissolved in a small amount of Milli-Q water and dialyzed against Milli-Q water for 3 days using a dialysis membrane with a MWCO

of 1 kDa. The dialysis water was changed twice a day. After the dialysis, the polymer was freeze-dried and denoted as **PNIPAM-*N*$_3$ #4260**.

3.9. Synthesis of *alkynyl*-CMC and *alkynyl*-CNF

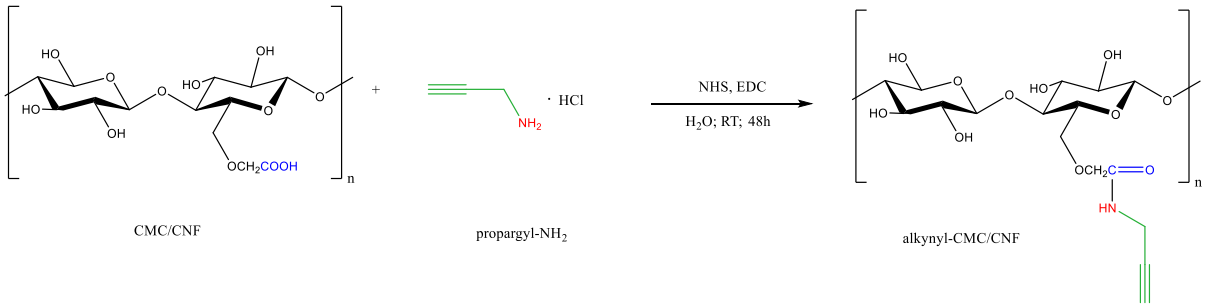

Figure 15. Synthetic route for preparation of *alkynyl*-CMC/CNF.

The precursors for the click reaction, *alkynyl*-CMC and *alkynyl*-CNF, were prepared by the amidation of celluloses with propargyl-*NH*$_2$ in the presence of EDC/NHS.

***Alkynyl*-CMC** was prepared as follows: CMC (0.2 g; 0.92 mmol) was predissolved in 40 mL water. NHS (0.127 g; 1.1 mmol) was charged into the flask and the solution was stirred for 30 min. Then, EDC (0.352 g; 1.8 mmol) was added to the reaction mixture and the solution was stirred for 90 more min. Reaction was started by adding propargyl-*NH*$_2$ (0.043 g, 0.47 mmol; in 2 mL water). The reaction was conducted at room temperature under stirring for 46 h. To remove impurities, the polymer solution was dialyzed (MWCO = 3.5 kDa) against water for 5 days and freeze-dried.

***Alkynyl*-CNF** was prepared as follows: 4.67 g wet CNF (0.07 g dry CNF) was first diluted with 7.5 ml water. NHS (0.062 g; 0.54 mmol; in 0.5 mL water) was charged into the flask and the solution was stirred for 30 min. Then, EDC (0.177 g; 0.92 mmol; in 0.5 mL water) was added to the reaction mixture and the solution was stirred for 90 more min. The reaction was started by adding propargyl-*NH*$_2$ (0.004 g, 0.04 mmol; in 0.5 mL water). The reaction was conducted at room temperature under stirring for 48 h. To remove impurities, the polymer solution was dialyzed (MWCO = 3.5 kDa) against water for 5 days. In order to prevent redispersion problems, *alkynyl*-CNF was used for further modification without freeze-drying.

3.10. Synthesis of CMC and CNF graft copolymers via click chemistry

The click chemistry route used in this work to graft polymer chains onto CMC and CNF is schematically illustrated in Figure 16 and Figure 17Figure 17. Synthetic route for preparation of CMC/CNF-*g*-PNIPAM #click.. In the first step, the carboxylic acid groups of CMC/CNF are propargylated by reductive amination with propargylamine hydrochloride. In the second step, the modified CMC/CNF is reacted with azide-modified polymers in the presence of Cu(ll) catalyst.

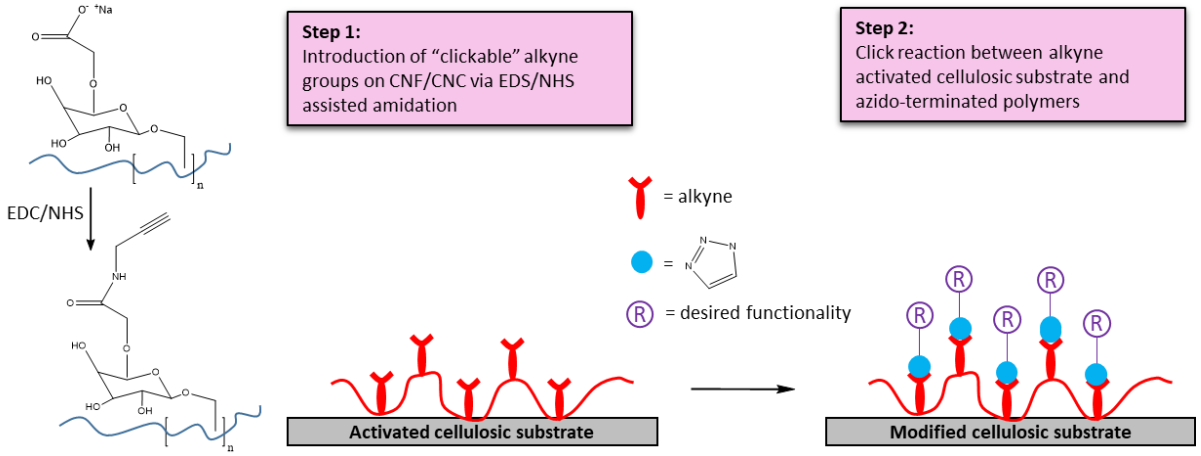

Figure 16. Schematic route for chemical modification of CMC/CNF with thermo-responsive polymers via Cu-catalyzed azide/alkyne cycloaddition (CuAAC).

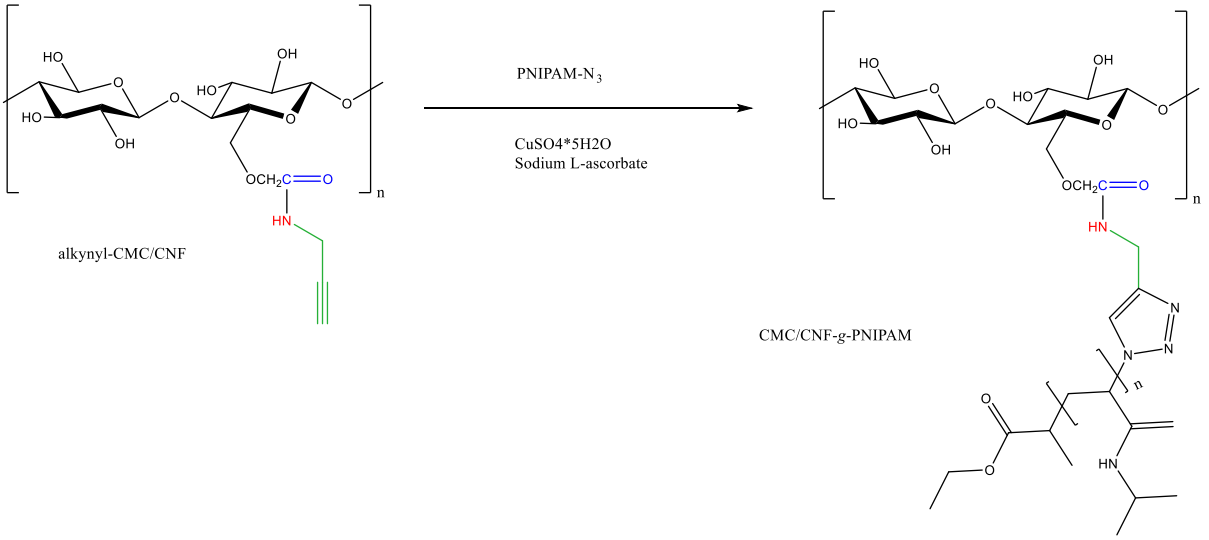

Figure 17. Synthetic route for preparation of CMC/CNF-*g*-PNIPAM #click.

CMC-*g*-PNIPAM #click was prepared as follows: *alkynyl*-CMC (0.0188 g; ≈ 0.08 mmol) and PNIPAM-N_3 #4260 (0.344 g; ≈ 0.08 mmol) were dissolved in 10 mL 0.1 M HCl and degassed with nitrogen. Under nitrogen atmosphere, $CuSO_4 \cdot H_2O$ (0.060 g; 0.24 mmol; in 1 mL of water) and sodium L-ascorbate (0.237 g; 1.2 mmol; in 1 mL of water) were added. Then, the pH value of the solution was adjusted to about 6.5 (0.1 M NaOH). At this point, the color of the mixture already switched from yellow to red-brown meaning that copper had most likely been oxidized to elementary copper. The mixture was stirred for 24 h at room temperature. The product was dialyzed (MWCO = 12-14 kDa) against 0.1 % acetic acid for 1 day until the product became transparent, then against Milli-Q water for 5 days and freeze-dried.

CNF-*g*-PNIPAM #click was prepared as follows: *alkynyl*-CNF (all) and PNIPAM-N_3 Sigma-Aldrich (0.3 g, 0.06 mmol; in 2 mL of water) were diluted with 3 mL 0.1 M HCl. At this point pH was 2.0. Then, $CuSO_4$ H_2O (0.075 g; 0.3 mmol; in 1 mL of water) and sodium L-ascorbate (0.298 g; 1.5 mmol; in 1 mL of water) were added. Then, the pH value of the solution was adjusted to about 6.0 (0.1 M NaOH) and the mixture was degassed with nitrogen. The yellow/orange-colored mixture was stirred for 24 h at room temperature. After 1 h, the color of the mixture olive-green. After a few more hours, the color was red-brown. The red/brown-colored product was dialyzed (MWCO = 12-14 kDa) against 0.1 % acetic acid for 1 day until the product became transparent, then against Milli-Q water for 5 days and partially freeze-dried. The freeze-dried sample was analyzed with ATRIR and the never-dried sample was analyzed with UV-VIS and DLS.

4. RESULTS & DISCUSSION

4.1. Synthesis of PDEGMA-NH_2 and PNIPAM-N_3

Low-molecular-weight polymer chains of PDEGMA-NH_2 and PNIPAM-N_3 were synthesized via ATRP. The synthesis of PDEGMA-NH_2 was started from an amine-terminated ATRP initiator, whereas PNIPAM was modified after polymerization to reach the azide termination. During the polymerizations, a few drops were periodically taken out of the reaction and analyzed by ^{1}H NMR in $CDCl_3$. Figure 18 shows the ^{1}H NMR spectra obtained at different times of the reactions. PDEGMA polymerization and purification were monitored by the disappearance of the monomer peak at 6.099 ppm and the appearing polymer peaks at 1.03 and 0.87 ppm. The conversion of NIPAM was determined by comparing the disappearing monomer peak at 5.5 ppm with the PNIPAM isopropyl peak at 4.1 - 3.9 ppm. The polymer purification by dialysis was considered as successful when the monomer peaks disappeared.

By integrating the peaks, the monomer conversion was calculated and plotted against the time (Figure 19). The theoretical values of polymer molecular weights (MW) were calculated from the conversions and the monomer to initiator ratios. It can be seen that the conversion rose rather linearly with the time until it reached a plateau above 90 % which proved that ATRP is a good method to synthesize polymers with controlled molecular weight.

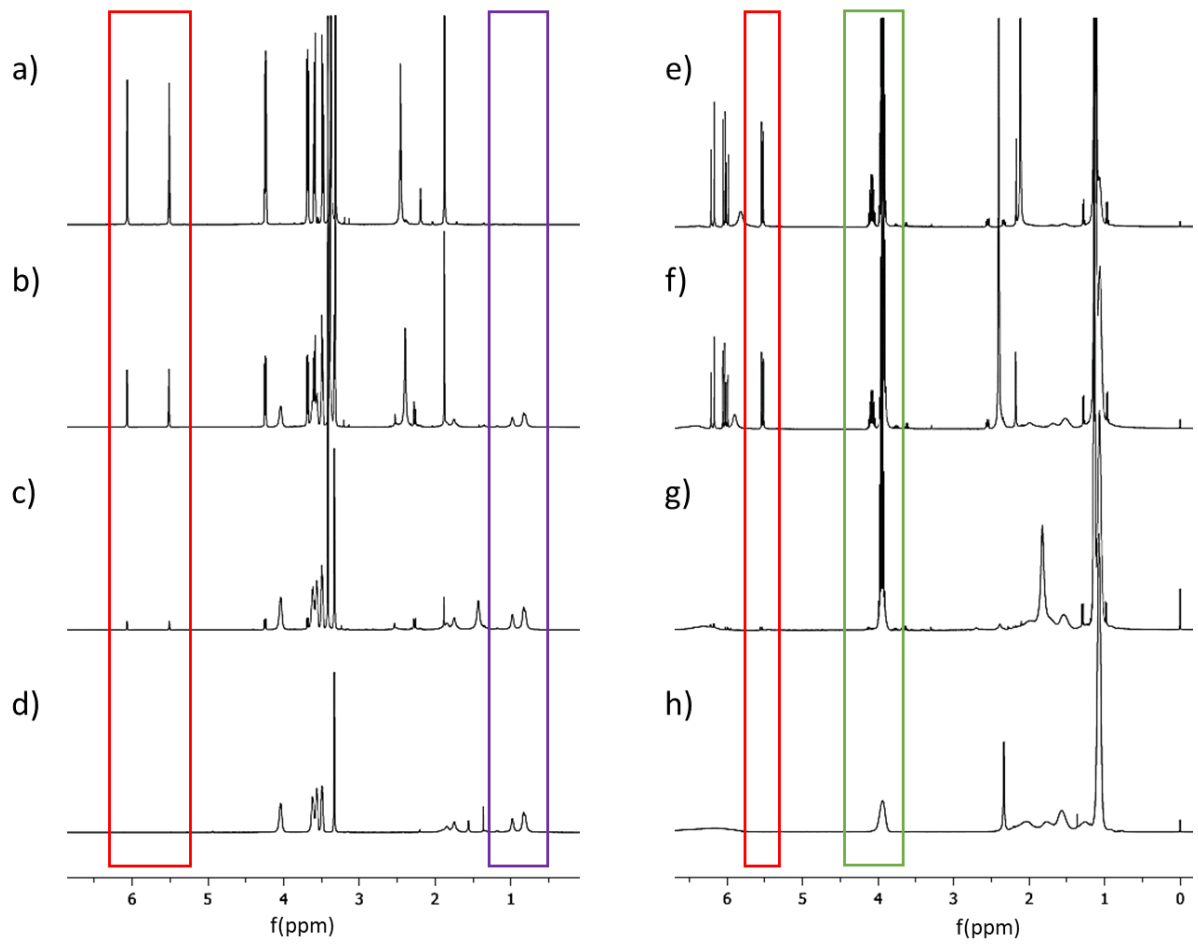

Figure 18. ^{1}H NMR spectra in $CDCl_3$ at RT – PDEGMA-*NH_2 (a)* at the beginning of the reaction, *(b)* after 80 min, *(c)* at the end of the reaction after 220 min, *(d)* after dialysis and freeze-drying; PNIPAM-*Cl (e)* at the beginning of the reaction, (f) after 2.5 h, (g) at the end of the reaction after 47 h, (h) after dialysis and freeze-drying.

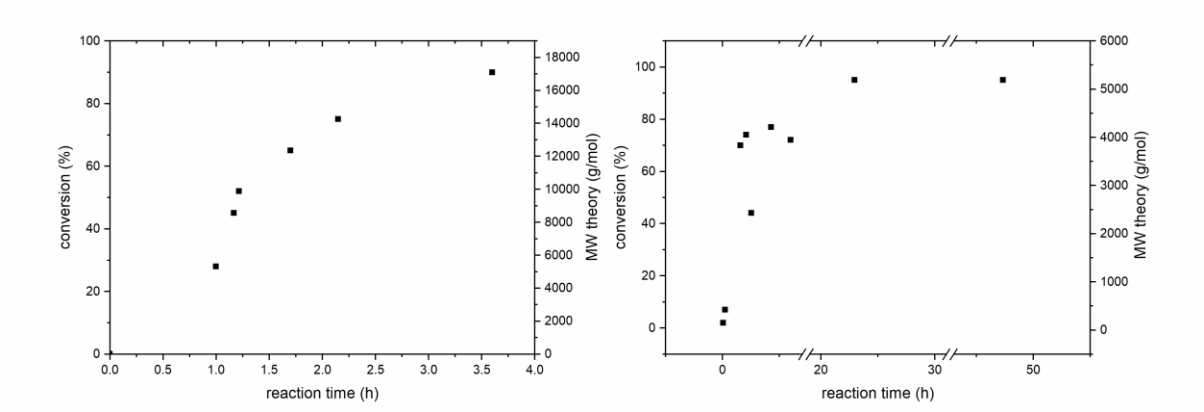

Figure 19. Monomer conversion (%) versus reaction time for ATRP of *(left)* PDEGMA-*NH_2* and *(right)* PNIPAM-*Cl*.

4.2. Thermo-responsive behavior of PDEGMA-NH_2 and PNIPAM-N_3

Thermo-responsive properties of the synthesized PDEGMA and PNIPAM were demonstrated by the example of PDEGMA-NH_2 #1 and PNIPAM-N_3 #4260 using DLS and UV-VIS spectroscopy. Figure 20 shows the DLS scans of the polymers.

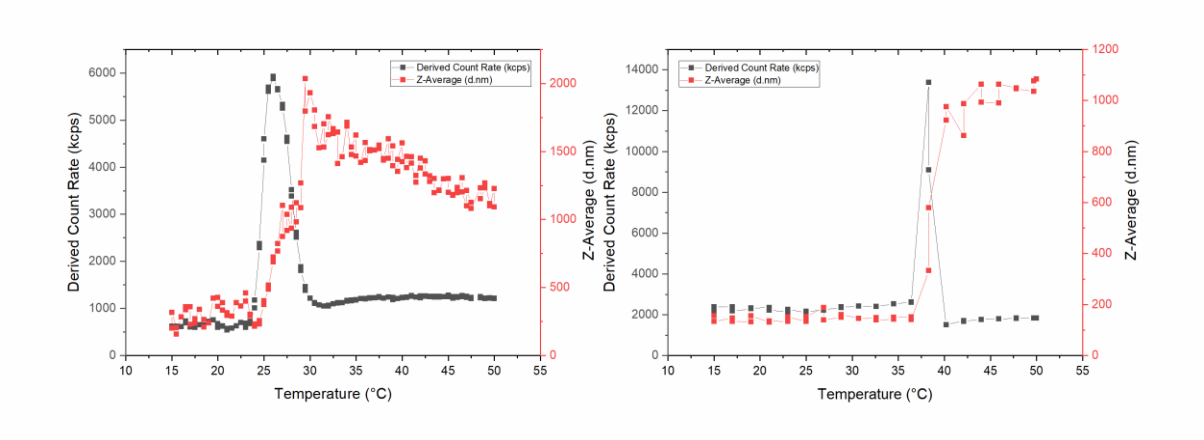

Figure 20. DLS of *(left)* PDEGMA-NH_2 #1 and *(right)* PNIPAM-N_3 #4260.

For PDEGMA-NH_2#1, the z-average size was below 500 nm below 25 °C. At 25 °C the size clearly began to grow until it reached a maximum of 2000 nm at 30 °C and then gradually started to decrease with increasing temperature. The count rate for this sample fluctuated in a range 500-700 kcps below 25 °C. At 25 °C it quickly rose to reach a maximum of 6000 kcps and with increasing temperature stabilized at around 1200 kcps. Thus, 25 °C was the LCST of this polymer solution which is in agreement with the literature. [1]

For the PNIPAM-N_3 sample, the size stayed constant under 200 nm below 37 °C; at 37 °C it started to gradually increase until it reached a plateau again at around 1000 nm. The count rate stayed constant at 2300 kcps below 37 °C; at 37 °C it jumped to reach the maximum value of 13000 kcps and then swiftly dropped back to 1800 kcps. Thus, 37 °C was the LCST of this polymer solution which is also in agreement with the literature [48].

Figure 21 shows the UV transmittance of the two selected polymers, measured at a constant wavelength of 500 nm and as a function of the measurement temperature. At the point of transition from a monophasic to a biphasic system, the solutions of PDEGMA-NH_2 and PNIPAM-N_3 became turbid due to light scattering caused by the phase separation. The turbidity

was quantified by UV-VIS. Below the LCST, both polymer solutions stayed transparent with a transmittance of over 90 %. Above the LCST, they both turned opaque with a transmittance below 0.5 %. However, according to these results, the LCSTs of the polymers are slightly higher than those measured with DLS – around 28 °C and 40 °C for PDEGMA-NH_2 and PNIPAM-N_3, respectively. This is due to inaccuracy of temperature control of the cell. Hence, the solution inside the cell never reached the temperature value shown on the instrument display (error circa -2 °C). Therefore, the UV-VIS transmittance results cannot be used to directly quantify the LCST of a solution but to assess its approximate value and observe the change in turbidity with increasing temperature. The transmittance drop from 90 % to 0.5 % is very sharp indicating that the phase change does not occur over the range of temperatures but rather happens at one certain temperature.

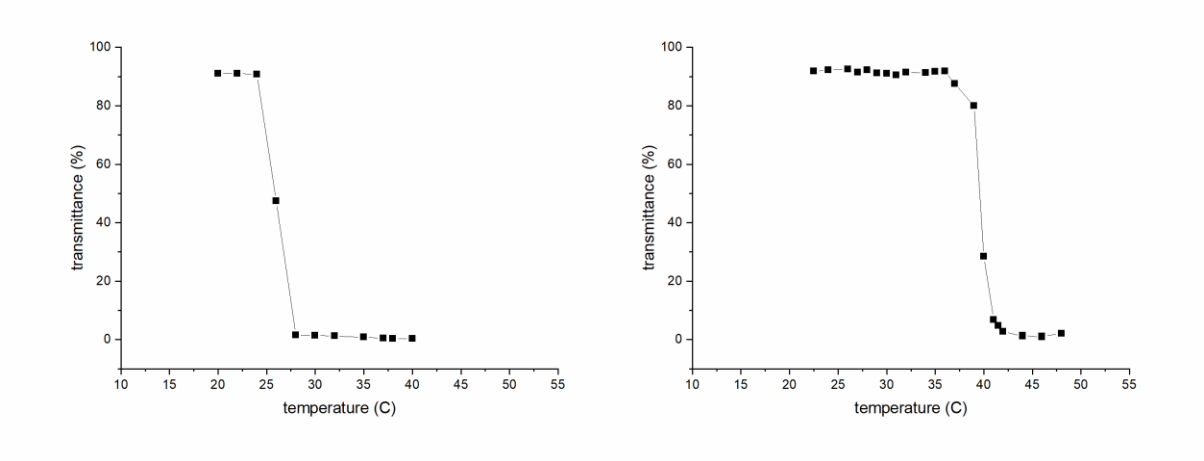

Figure 21. UV-VIS transmittance at 500 nm of *(left)* PDEGMA-NH_2 #1 and *(right)* PNIPAM-N_3 #4260.

4.3. Synthesis of CMC and CNF graft copolymers via EDC/NHS chemistry

CMC and CNF graft copolymers were synthesized via EDC/NHS chemistry. CNF based hydrogels could not be redispersed after freeze-drying. Hence, they were never dried and their exact concentration in water was unknown. CMC based hydrogels did not show any redispersion problems.

The grafting densities of the polymer chains had to be low enough to ensure the gelling behavior of the cellulose hydrogels but high enough to show some thermal response. For modified CMC samples, 10, 30 and 50 % of the available carboxylic acid groups were aimed

to be linked with PNIPAM in CMC-*g*-PNIPAM #1, #2, and #3, respectively. In the CMC-*g*-PDEGMA sample, ≈1 % of the carboxylic acid groups were aimed to be bound with PDEGMA. In the CNF-*g*-PNIPAM #1, #2, #3 and CNF-*g*-PDEGMA samples, 30, 50, 100 and ≈11 % of the available carboxylate groups were aimed to be bound with the thermo-responsive polymer chains. The modification of CMC and CNF was assessed by comparing the ATR-IR spectra of unmodified and modified CMC and CNF.

The infrared spectrum of CMC (Figure 22a) showed a broad band at 3600-3000 cm^{-1}, attributed to O-H stretching vibration; a peak at approximately 2900 cm^{-1} due to the stretching frequency of the C-H groups. The peak at 1588 cm^{-1} was assigned to the asymmetric stretching vibration of the carboxylate groups. The peak at 1417 cm^{-1} can be attributed to both -CH_2 scissoring and COO^- symmetric stretching vibration. The peak at 1315 cm^{-1} was ascribed to O-H bending vibration. The intense absorption band at 1200-900 cm^{-1} can be attributed to the ether groups from the polysaccharide.[34]

The infrared spectrum of PNIPAM-NH_2 (Sigma Aldrich) (Figure 22e) displayed a peak at 3294 cm^{-1} due to the N-H stretching vibration. The peaks at 2970, 2931 and 2875 cm^{-1} can be related to the axial deformation of C-H groups. Amide I and amide II stretching vibrations were found at 1637 and 1534 cm^{-1}, respectively. The peak at 1457 cm^{-1} can be attributed to CH_3 antisymmetric bending, CH_2 scissoring and C-N stretching of amide groups. The peaks at 1385, 1366 cm^{-1} were assigned to the symmetric bend (or umbrella bend) of isopropyl groups of PNIPAM. [34]

All the CMC-*g*-PNIPAM copolymers spectra (Figure 22b-d) displayed the characteristic absorptions of PNIPAM, such as the peaks of amide I (~1640 cm^{-1}), amide II (~1533 cm^{-1}) and isopropyl groups (1385 and 1365 cm^{-1}). Besides, they also exhibited the bands of CMC, such as O-H bending vibration (~1315 cm^{-1}); -CH_2 scissoring and COO^- symmetric stretching vibration (~1417 cm^{-1}); and the broad peak at ~1030 cm^{-1}, due to the ether groups from CMC.

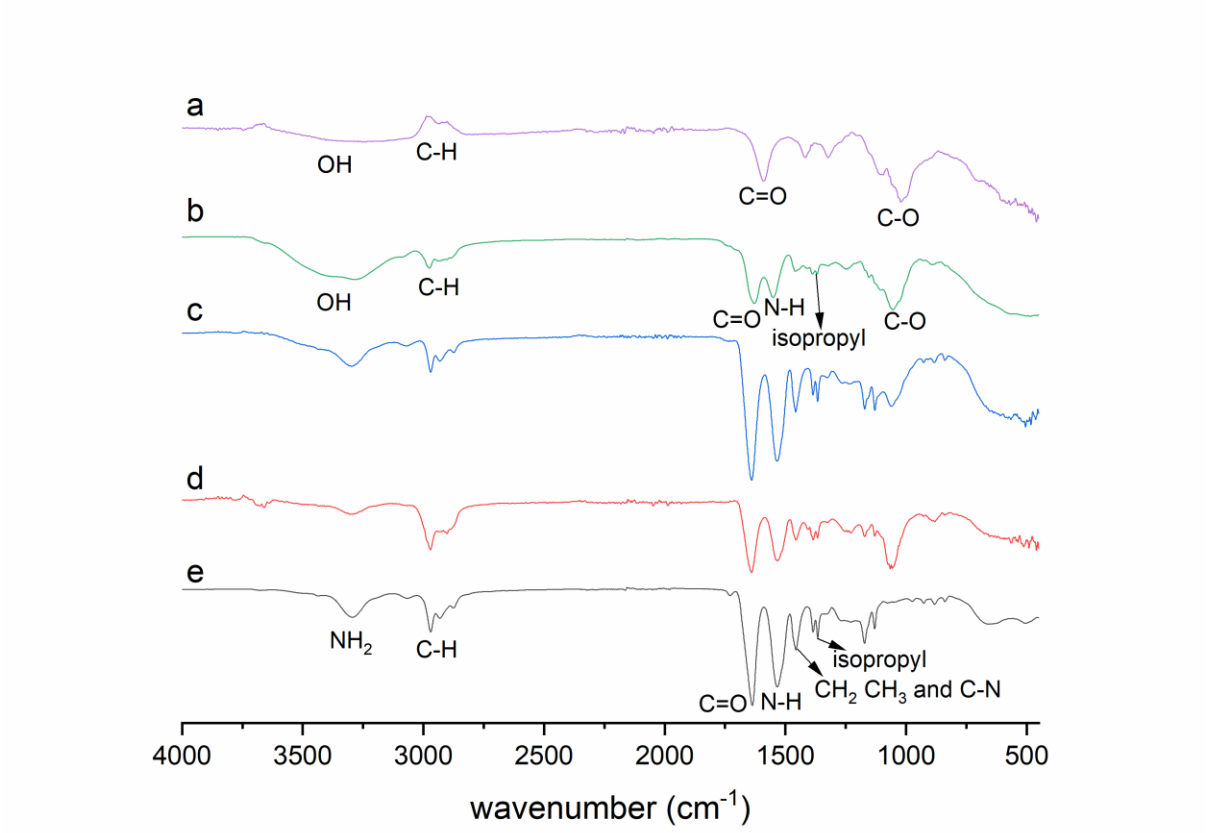

Figure 22. ATR-IR absorption spectra of *(a)* CMC, *(b)* CMC-*g*-PNIPAM #1, *(c)* CMC-*g*-PNIPAM #2, *(d)* CMC-*g*-PNIPAM #3, and *(e)* PNIPAM-NH_2 (Sigma Aldrich).

The infrared spectrum of CNF (Figure 23a) is to a certain extent similar to the one of CMC. Three cellulose-related bands were identified at 3600-3000 cm^{-1}, assigned to O-H stretching; at ~2900 cm^{-1}, assigned to C-H stretching; and at 1057-1032 cm^{-1}, assigned to C-O stretching. The peak observed at 1613 cm^{-1} was assigned to COO^- stretching in sodium form.

All the CNF-*g*-PNIPAM copolymers spectra displayed the characteristic absorptions of PNIPAM and CNF.

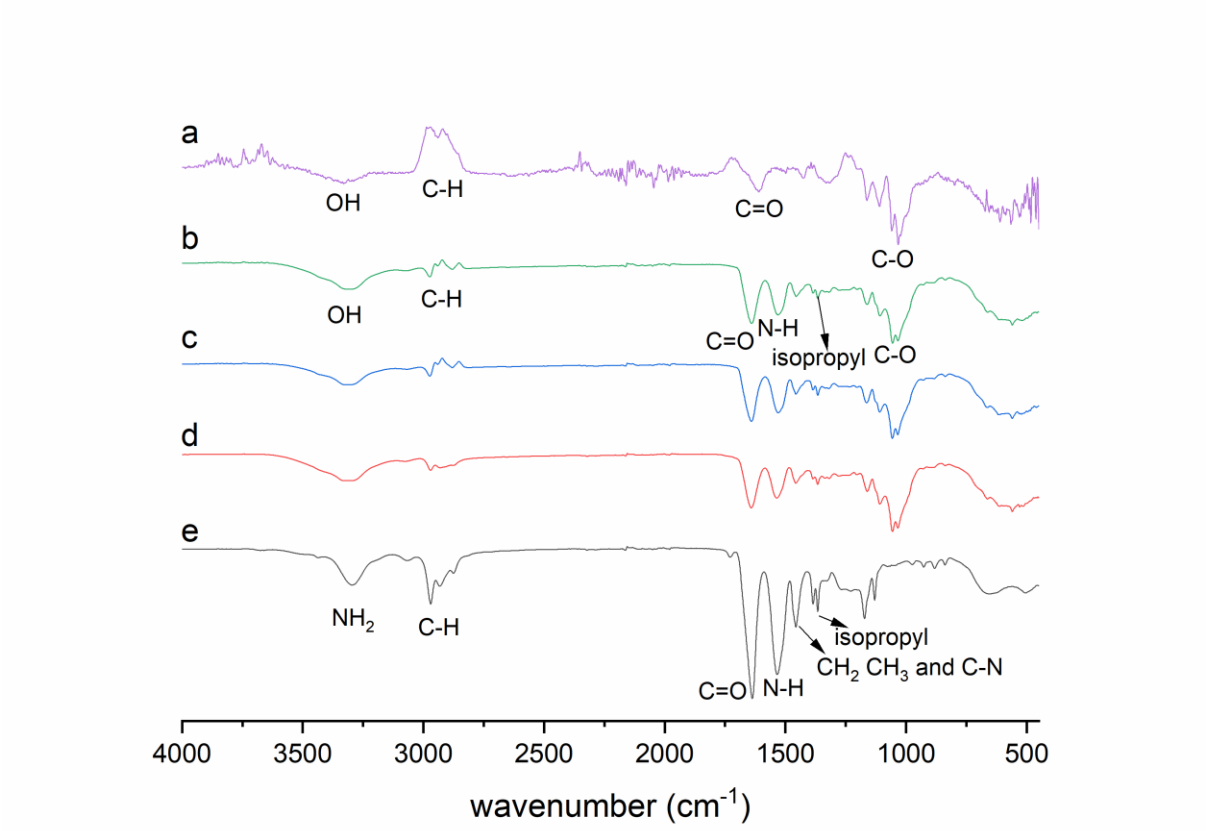

Figure 23. ATR-IR absorption spectra of *(a)* CNF, *(b)* CNF-*g*-PNIPAM #1, *(c)* CNF-*g*-PNIPAM #2, *(d)* CNF-*g*-PNIPAM #3, and *(e)* PNIPAM-NH_2 (Sigma Aldrich).

Figure 24 shows the IR spectra of CMC, CMC-*g*-PDEGMA and PDEGMA #1. In the IR curve of CMC-*g*-PDEGMA, a peak corresponding to the carbonyl stretching, attributed to the ester group in PDEGMA, appears at 1725 cm^{-1}, clearly showing the presence of PDEGMA. Furthermore, absorption bands of CMC were observed in the same sample. Peaks at around 3300, 1590 cm^{-1} correspond to hydroxyl and carboxyl groups of CMC, respectively; they are not visible in the spectrum of pure PDEGMA-NH_2. The stretching vibration bands of C-O bonds in CMC, CMC-*g*-PDEGMA and PDEGMA #1 are at 1015, 1065 and 1100 cm^{-1}, respectively, with CMC-g-PDEGMA being right in the middle.

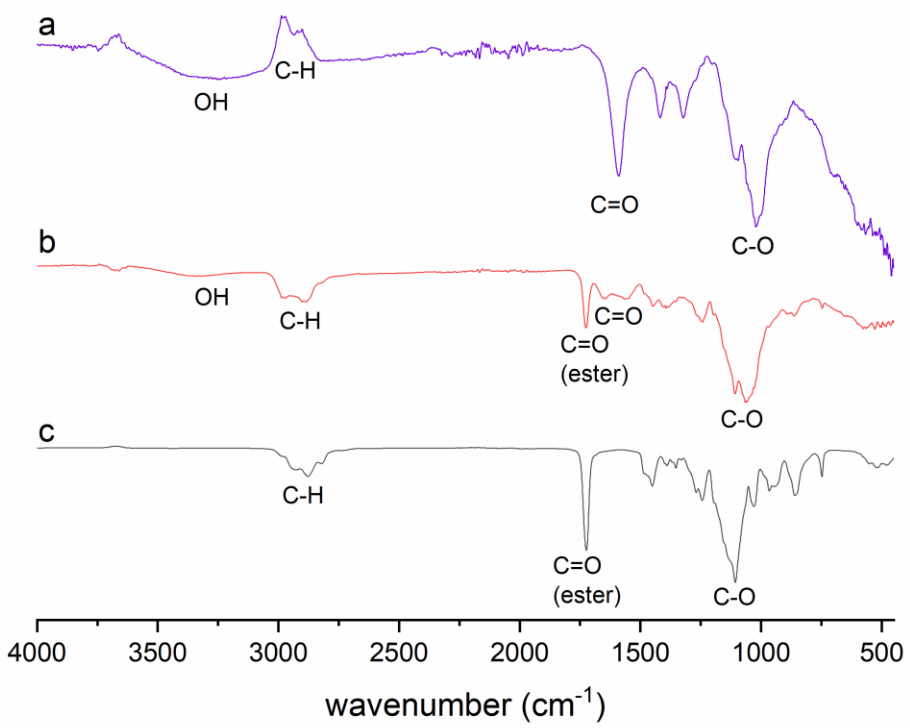

Figure 24. ATR-IR absorption spectra of *(a)* CMC, *(b)* CMC-*g*-PDEGMA and *(c)* PDEGMA-NH_2 #1.

Figure 25 illustrates the IR spectra of CNF-g-PDEGMA and PDEGMA #2. The IR curve of PDEGMA #2 is very similar to the one of PDEGMA #1 showing a distinctive ester group peak at 1725 cm^{-1}. The spectrum of CNF-g-PDEGMA clearly has the same peak as well as others from the CNF spectrum, such as bands of hydroxyl and carboxyl groups of CNF at around 3300, 1590 cm^{-1}.

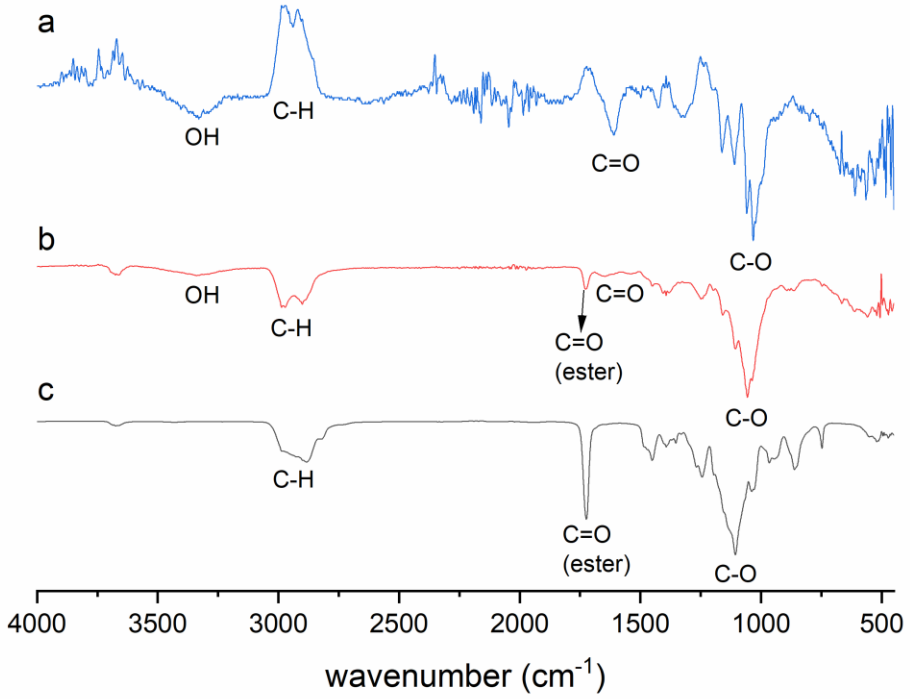

Figure 25. ATR-IR absorption spectra of *(a)* CNF, *(b)* CNF-*g*-PDEGMA and *(c)* PDEGMA-NH_2 #2.

Unfortunately, presence of PNIPAM and PDEGMA peaks in the spectra of copolymers does not necessarily prove their covalent grafting but mainly the presence or absence of PNIPAM/PDEGMA. The adsorption of polyelectrolytes or charged oligomers onto carboxymethyl groups of different cellulose derivatives has been widely shown.[27] In some cases, it seems even possible to have irreversible adsorption and no desorption in spite of multiple washing steps. Adsorption of amine-terminated PNIPAM on TEMPO CNCs has already been observed by Gicquel et al. (2019).[27] In spite of several purification methos, it was difficult for them to distinquish between surface adsorbtion and covalent grafting on the charged CNCs.

4.4. Adsorption vs chemical grafting

In order to investigate whether PNIPAM was adsorbed rather than covalently attached on both CMC and CNF, the polymer was mixed with the celluloses, stirred for 48 h. The polymer was then purified firstly with a 3.5 kDa MWCO membrane, then with a 12-14 kDa MWCO membrane, and after that mixed with excess 0.2 M KCl and dialyzed with a 12-14 kDa MWCO

membrane again. Figure 26 and Figure 27 show the ATR-IR spectra of the freeze-dried PNIPAM-adsorbed samples. For both CMC-*ads*-PNIPAM and CNF-*ads*-PNIPAM, the isopropyl peak at 1385-1365 cm^{-1} was visible after all purification steps indicating the presence of PNIPAM. Therefore, PNIPAM tends to adsorb onto CMC and CNF and PNIPAM in CMC/CNF-*g*-PNIPAM samples might as well only be adsorbed and not chemically bound.

None of the used purification methods removed PNIPAM completely. Future studies could investigate other purification methods, such as using a higher concentrated potassium chloride solution or adjusting pH of the sample to 2-3 prior to dialysis.

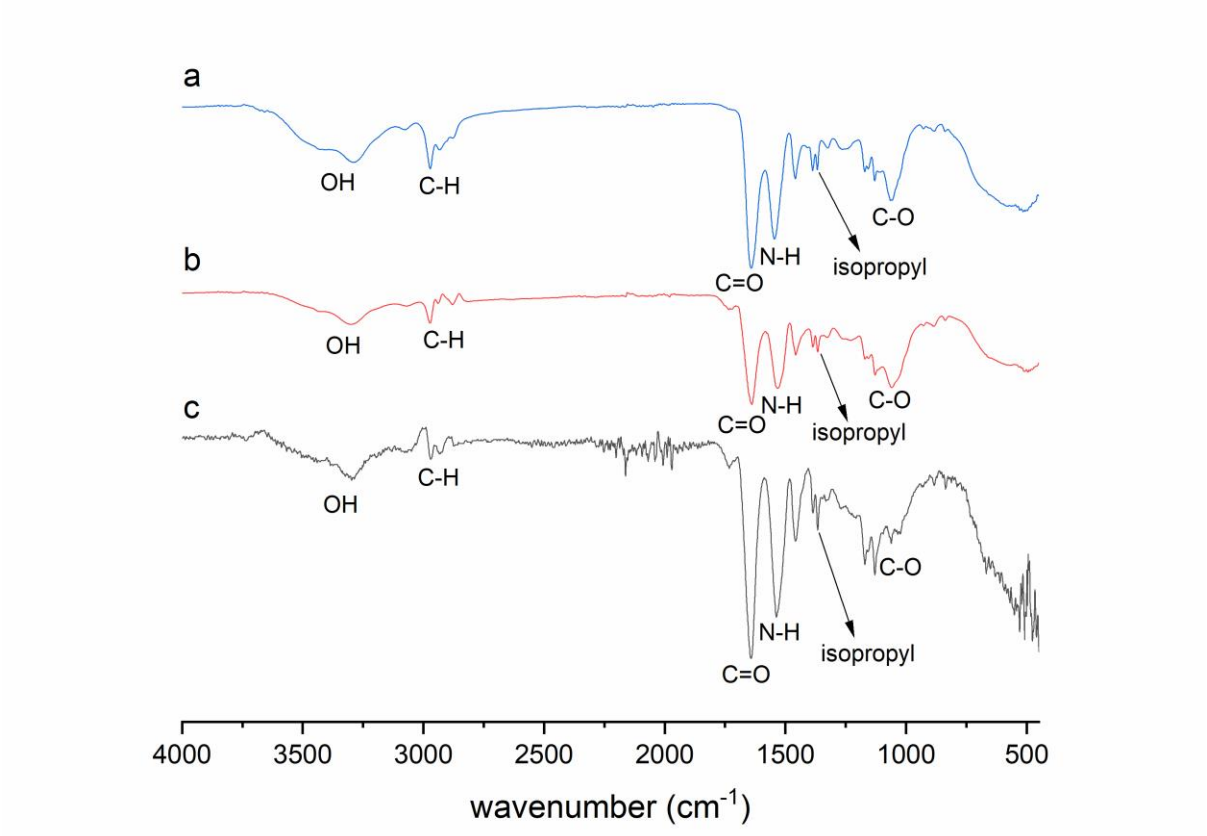

Figure 26. ATR-IR absorption spectra of freeze-dried CMC-*ads*-PNIPAM *(a)* after dialysis with 3.5 kDa membrane, *(b)* after dialysis with 12-14 kDa membrane, *(c)* after mixing with 0.2 M KCl and dialysis with 12-14 kDa membrane.

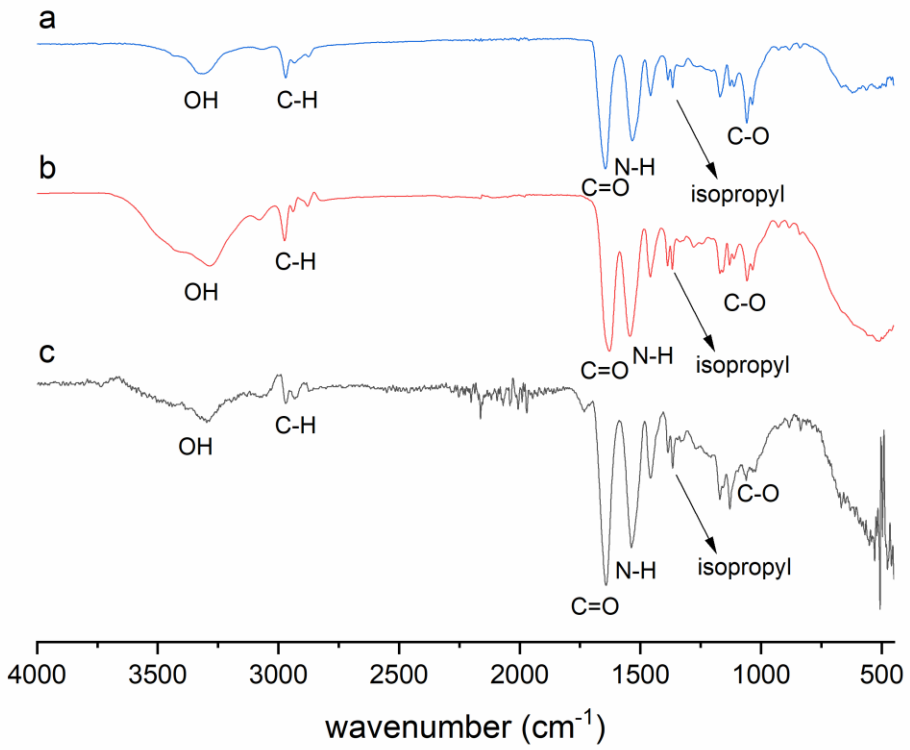

Figure 27. ATR-IR absorption spectra of freeze-dried CNF-*ads*-PNIPAM *(a)* after dialysis with 3.5 kDa membrane, *(b)* after dialysis with 12-14 kDa membrane, *(c)* after mixing with 0.2 M KCl and dialysis with 12-14 kDa membrane.

4.5. Synthesis of *alkynyl*-CMC and *alkynyl*-CNF

Alkynyl groups were introduced to CMC and CNF via EDC/NHS chemistry. For both *alkynyl*-CMC and *alkynyl*-CNF the aim was to modify half of the available carboxylic acid groups. The modification of CMC and CNF was assessed by comparing the ATR-IR spectra of unmodified and modified CMC and CNF.

In the ATRIR spectrum of the *alkynyl*-modified CMC shown in Figure 28, no absorbance peak at 2150-2100 cm^{-1} was found suggesting the unsuccessful introduction of alkynyl group on CMC backbone. However, two peaks appeared at 1650 and 890 cm^{-1} which could be due to N-H scissoring and N-H out-of-plane bending vibration, respectively [58]. Thus, even though the alkyne peak is too weak to be visible, the characteristic amide bands proved the grafting of alkynyl groups. In a similar way, from the ATRIR specrum of alkynyl-CNF shown in Figure 29b, the typical alkyne peak was not visible but the typical amide bands were found at 1650 and 890 cm^{-1}.

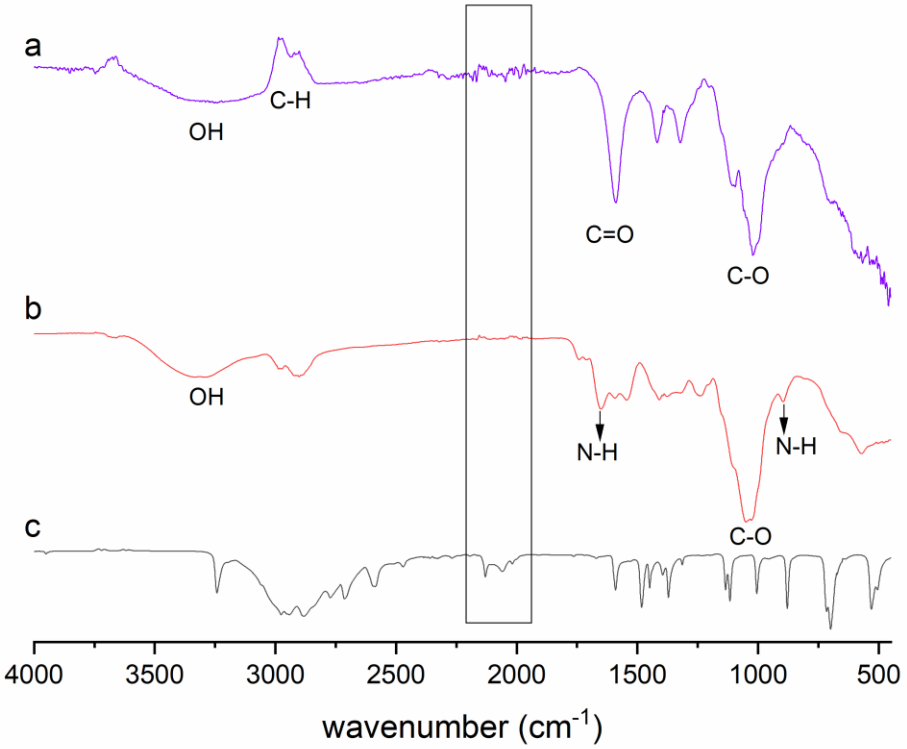

Figure 28. ATR-IR absorption spectra of *(a)* CMC, *(b) alkynyl*-CMC, *(c)* propargyl-NH_2.

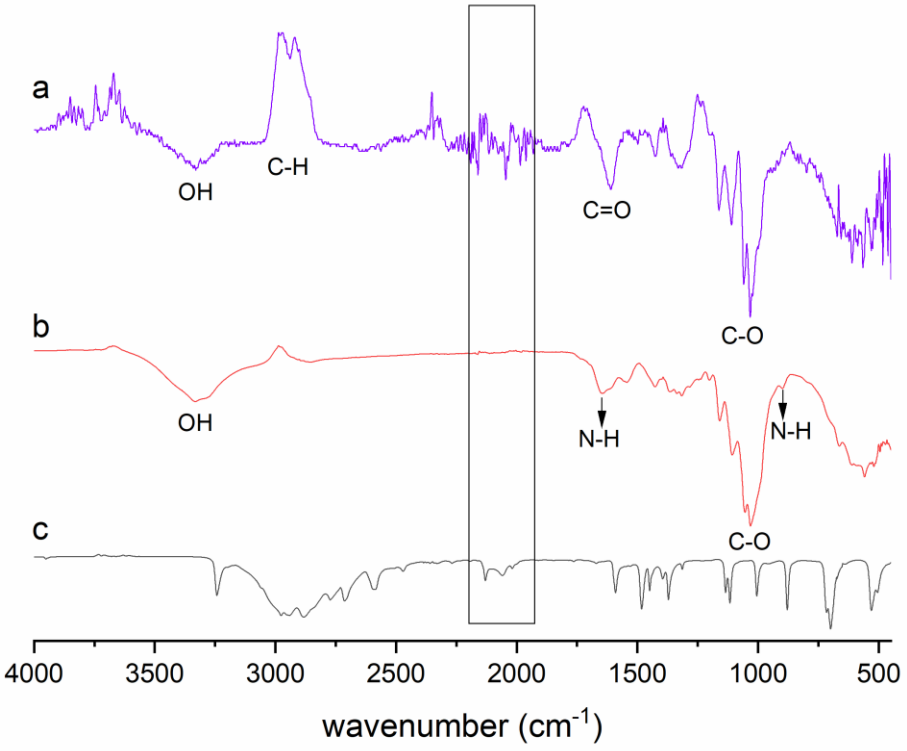

Figure 29. ATR-IR absorption spectra of *(a)* CNF, *(b) alkynyl*-CNF, *(c)* propargyl-NH_2.

4.6. Synthesis of CMC and CNF graft copolymers via click chemistry

The infrared spectra of CMC/CNF-*g*-PNIPAM #click and azido-terminated PNIPAM are shown in Figure 29 and Figure 30.

After PNIPAM-*Cl* had been synthesized, the chloride end group was attempted to be replaced with an azide group by mixing with NaN_3 in DMF. However, the desired azido peak at around 2100 cm^{-1} was not found and the end group substitution was considered unsuccessful at first. Therefore, PNIPAM-N_3 was ordered from Sigma-Aldrich and again there was no difference in the spectrum compared to PNIPAM-*Cl*. However, the azide IR peak could have been too weak to be seen. [58]

Similar to CMC and CNF graft copolymers synthesized via EDC/NHS chemistry, CMC-*g*-PNIPAM #click and CNF-*g*-PNIPAM #click spectra displayed the characteristic absorptions of PNIPAM, such as peaks of amide I (~1640 cm^{-1}), amide II (~1524 cm^{-1}) and isopropyl groups (1385 and 1365 cm^{-1}). Besides, they also exhibited the bands of cellulose, such as the broad peak at ~1000 cm^{-1}, due to the ether groups from CMC.

Since the azido and alkynyl groups at 2100 cm^{-1} were not visible, the covalent grafting could not be proven by the disappearance of the characteristic peaks. The bands of both CMC/CNF and PNIPAM only prove the presence of PNIPAM but not its covalent grafting.

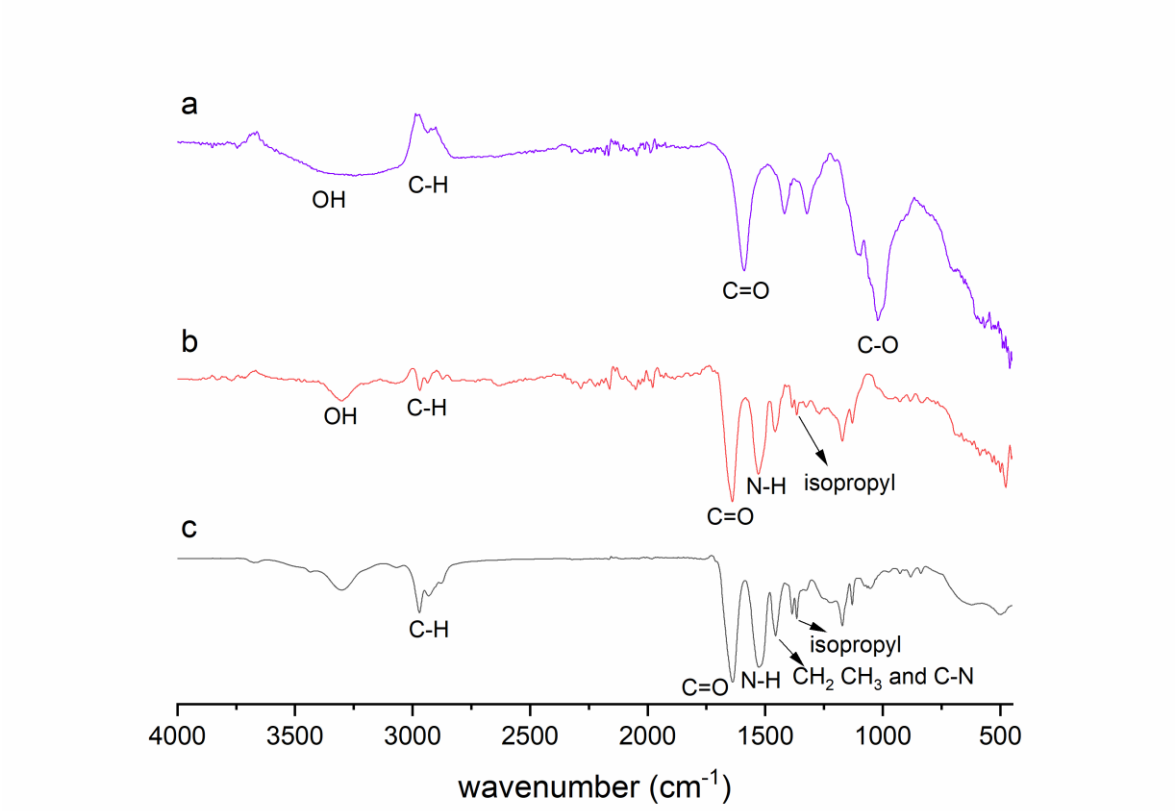

Figure 30. ATR-IR absorption spectra of *(a)* CMC, *(b)* CMC-*g*-PNIPAM #click, *(c)* PNIPAM-N_3 #4260.

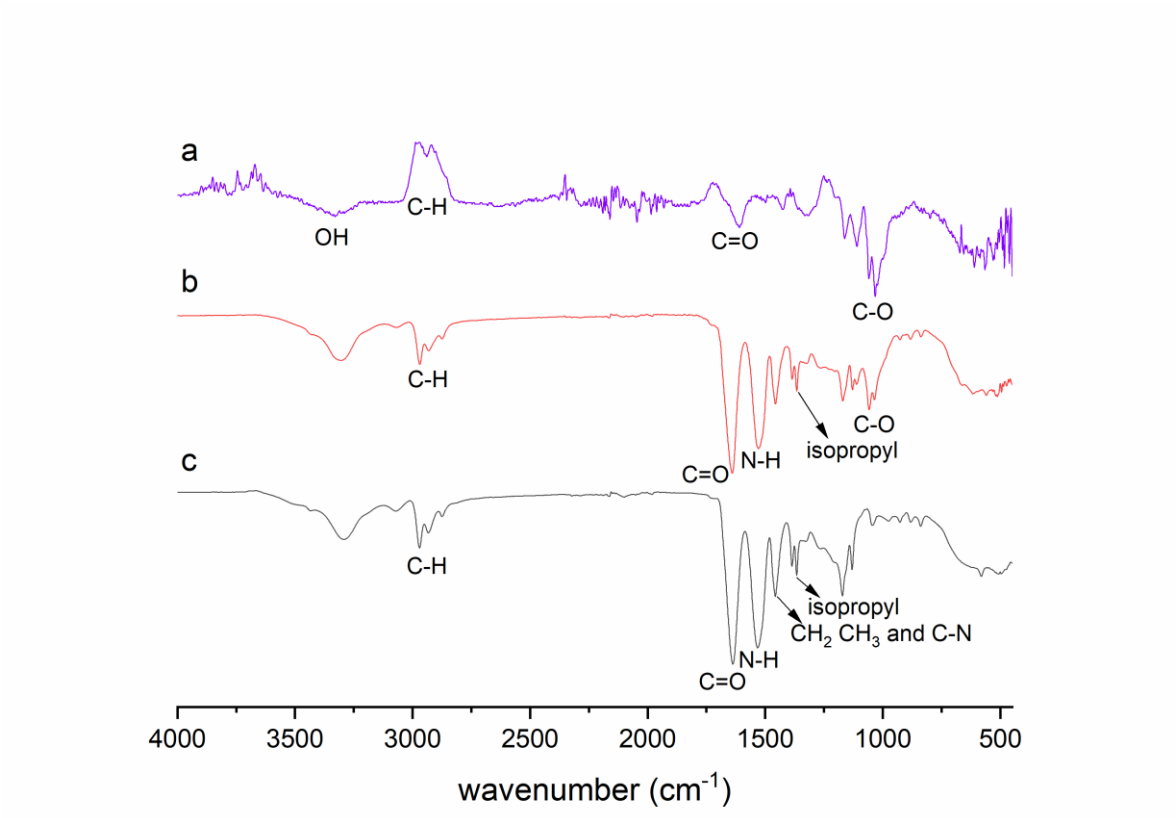

Figure 31. ATR-IR absorption spectra of *(a)* CNF, *(b)* CNF-*g*-PNIPAM #click, *(c)* PNIPAM-N_3 (Sigma Aldrich).

4.7. Thermo-responsive behavior of CMC and CNF graft copolymers

Modified and unmodified CMC and CNF were heated as a first check to show the thermal response. It can be seen from Figure 32 that both CMC and modified CMC are fully transparent at room temperature. Upon heating to 40 °C, the unmodified CMC solution remains clear, whereas the modified CMC turned white and completely opaque already proving the presence of thermal response. CNF is naturally slightly white and opaque but it does not change the color or transparency with increasing temperature. CNF modified with PNIPAM clearly became whiter and less transparent upon heating. The visual change in color was already a promising result and the thermo-responsive properties of the modified CMC and CNF were explored further with UV-VIS and DLS.

The change in turbidity was quantified by UV-VIS as shown in Figure 33. For pure CMC and CNF, no change in turbidity with the increasing temperature could be observed. CMC showed a transmittance over 90 % over the whole temperature range (20-50 °C). CNF is naturally slightly turbid; therefore, the transmittance was lower but stayed constant with increasing the temperature.

All the modified CMC and CNF samples showed a change in turbidity with increasing temperature. All CMC-*g*-PNIPAM samples were measured at the same concentration in water (1 mg/mL) and showed a sharp change in turbidity at 35-40 °C. The higher the amount of PNIPAM was added to CMC-*g*-PNIPAM samples, the lower the transmittance at higher temperatures was. This clearly proves that the temperature response comes solely from the grafted PNIPAM. It would be interesting to evaluate the lowest grafting density of PNIPAM which would be high enough for the sample to exhibit evidence of thermal response. CNF-*g*-PNIPAM samples also exhibited phase change at around 35-40 °C. However, the exact concentration of the modified CNF samples in water is unknown and not much comparison between the samples can be made. Both CMC-*g*-PDEGMA and CNF-*g*-PDEGMA underwent phase change at around 25 °C. Nonetheless, the exact LCST cannot be estimated with this method, as the temperature control is not precise.

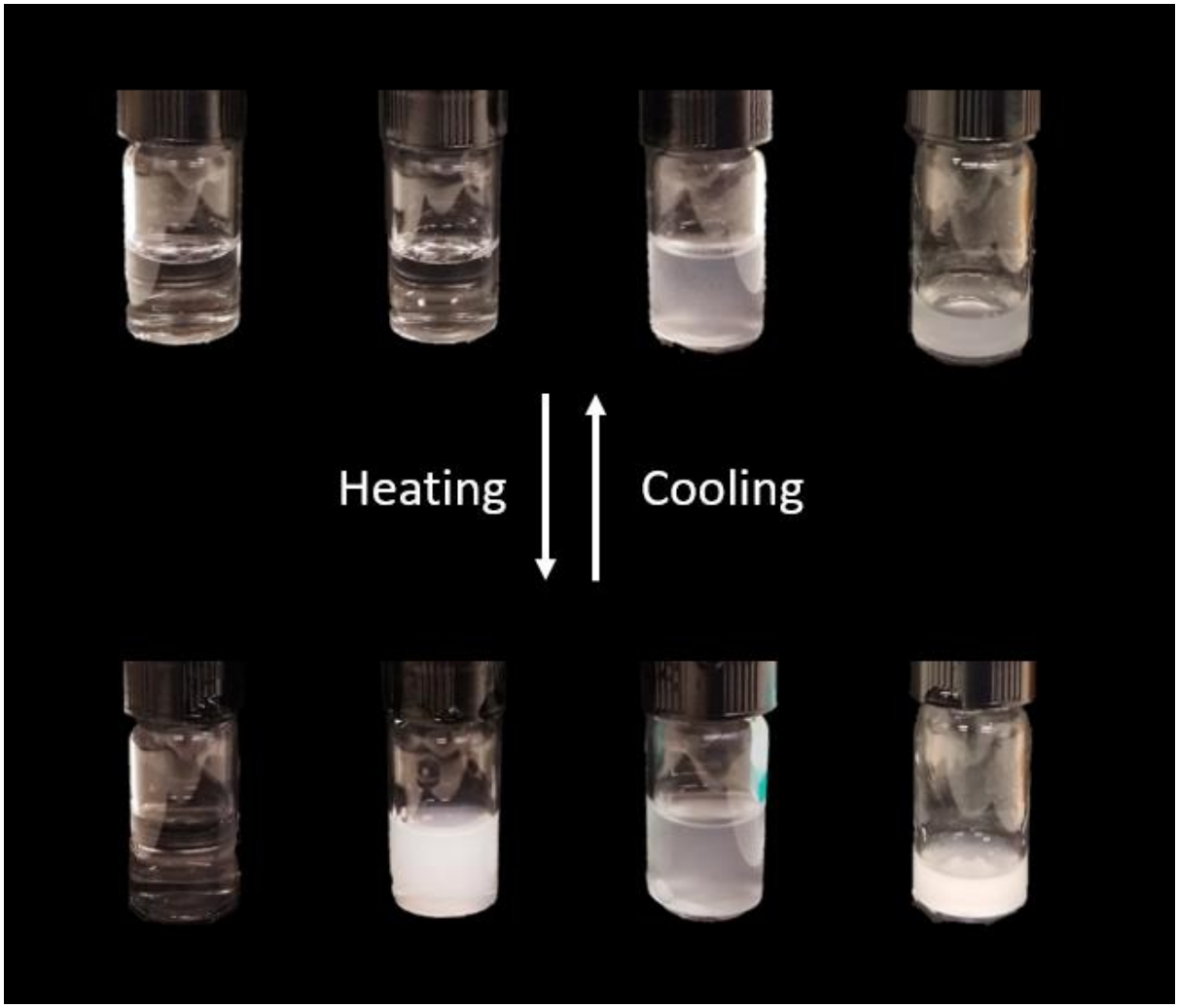

Figure 32. Temperature response of *(left to right)* 4.15 mg/mL CMC, 4.2mg/mL CMC-*g*-PNIPAM #2, 3.75mg/mL CNF, and never-dried (~3mg/mL) CNF-*g*-PNIPAM #2 aqueous solutions upon heating from room temperature to 40 ˚C.

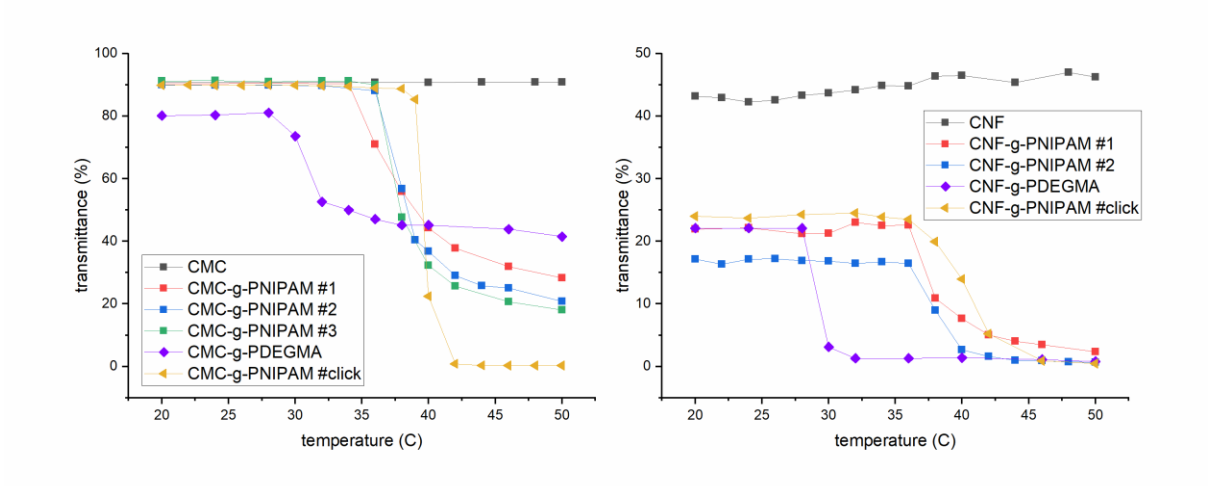

Figure 33. UV-VIS transmittance at 500 nm of *(left)* CMC and modified CMC water solutions (1 mg/mL) and *(right)* never-dried CNF and modified CNF water solutions (0.5-3 mg/mL).

As mentioned earlier in section (2.2.2), the aim of this work was to produce physically crosslinked hydrogels rather than chemically cross-linked. In physically crosslinked networks, the gelation transition is reversible after removing the gelling stimuli, aka temperature. In order to prove reversibility of the temperature response, CMC-*g*-PNIPAM #2 was measured with UV-VIS with a cycle repeated 3 times: heating from 20 to 50 °C, followed by cooling to 20 °C. As can be seen from Figure 34, the transmittance values stayed the same over the cycles.

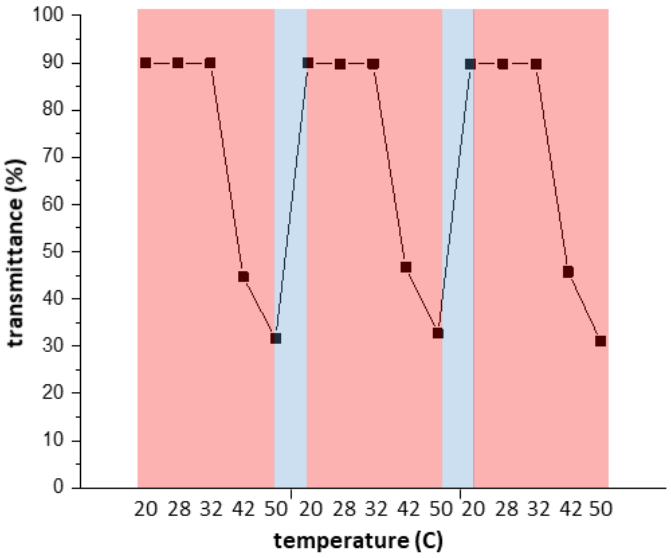

Figure 34. UV-VIS transmittance at 500 nm of CMC-*g*-PNIPAM #2 (1 mg/mL in water). Red area – heating from 20 to 50 °C, blue area – cooling from 50 to 20 °C.

DLS tests were carried out to prove the thermal response of the modified CMC and CNF once more and to quantify their LCSTs more precisely. In Figure 35, the hydrodynamic diameters of CMC and CNF were measured as function of temperature. Since the polymer chains in question are not spherical, the scattering of light is different depending on their orientation and the size value fluctuates a lot. For both CMC and CNF, a temperature change had no clear influence on the size of the particles or derived count rate.

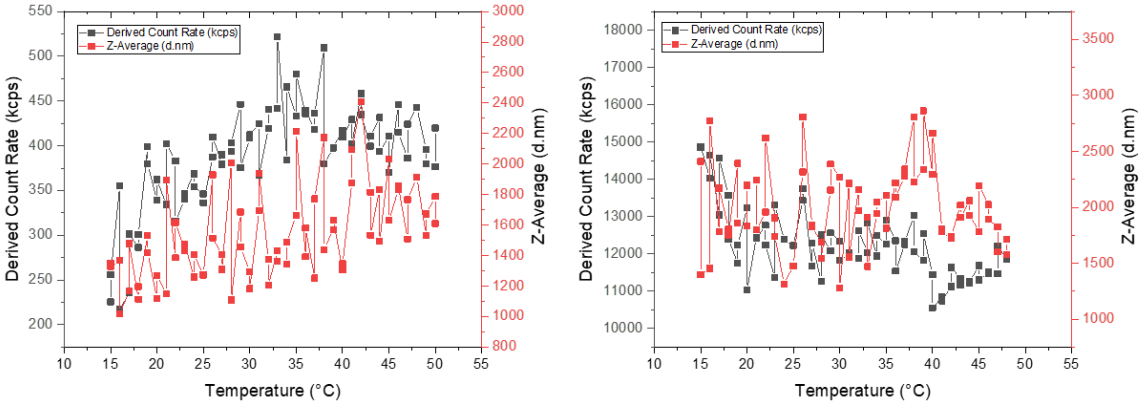

Figure 35. DLS of *(left)* CMC and *(right)* CNF water solutions (1 mg/mL).

Figure 36 shows the DLS curves for CMC and CNF modified with PNIPAM via EDC/NHS chemistry. For all the samples, the z-average diameter fluctuated significantly below 35 °C. Below 35 °C, the copolymers were relaxed polymer chains and the measured diameter of the equivalent sphere is simply meaningless. However, above 35 °C, the measured diameter stabilized at a constant value proving that there was a coil-to-globule transition and the measured particles became more spherical. Thus, the LCST for these samples was 35 °C and the phase change took place at the same temperature as with a water solution of PNIPAM-NH_2 (Sigma Aldrich) (Appendix 1). DLS is not a suitable method to determine the exact sizes of the copolymers chains but it clearly proves the difference in behavior with increasing temperature and helps to identify the LCSTs of the copolymers.

In the work of Gicquel et al. (2019), the same PNIPAM-NH_2 from Sigma Aldrich with the same MW was grafted onto TEMPO CNCs.[27] The thermal response of the modified CNCs was also proven with DLS. However, for some reason the phase transition occurred earlier, at around 30 °C. This might be explained by an inaccurate temperature control. Furthermore, their reported phase change was not sharp and did not occur at one specific temperature. The particle size rather gradually increased over the whole temperature range between 30 to 50 °C. The reason might be a too short equilibration time at every investigated temperature and, thus, an incomplete phase transition of the investigated solutions.

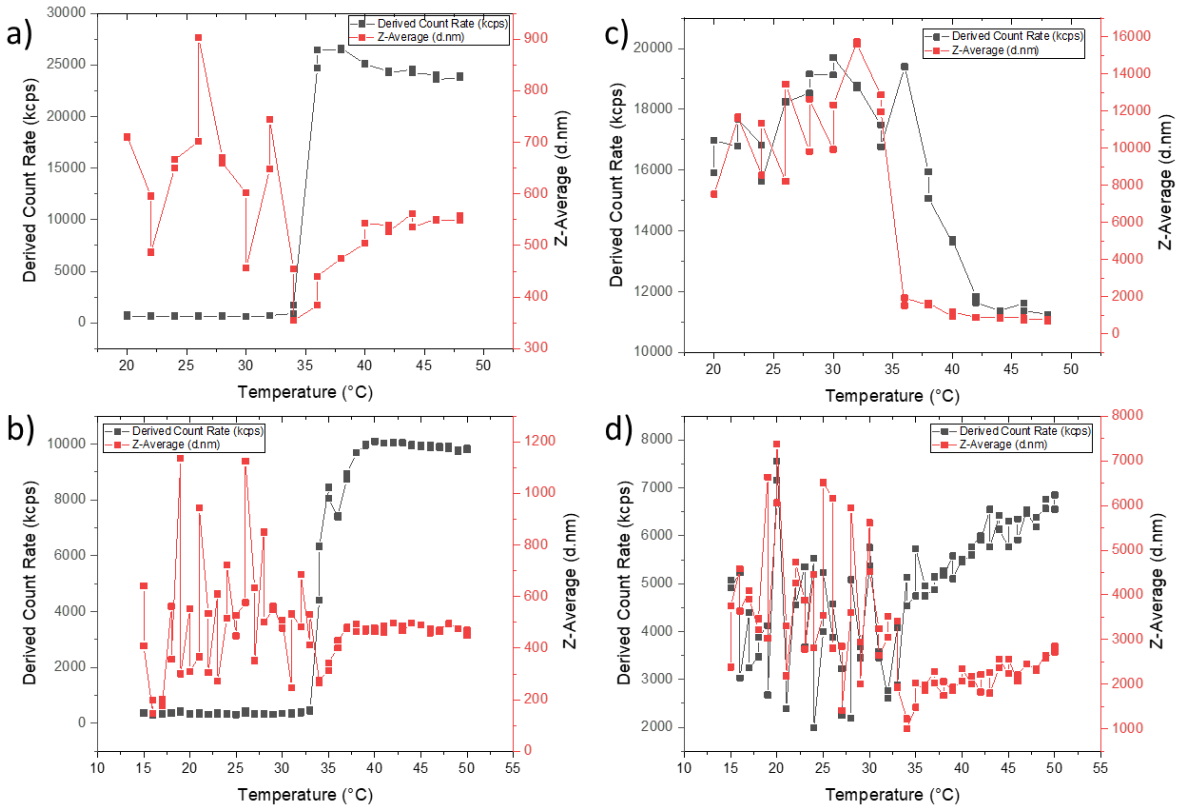

Figure 36. DLS curve for water solutions of a) CMC-*g*-PNIPAM #1 (1 mg/mL), b) CMC-*g*-PNIPAM #2 (1 mg/mL), c) CNF-*g*-PNIPAM #1 (never-dried, ~3 mg/mL), d) CNF-*g*-PNIPAM #2 (never-dried, ~3 mg/mL).

In order to prove reversibility of the temperature response, CMC-*g*-PNIPAM #2 was measured with DLS with a (heating to 50 ˚C - cooling to 20 ˚C) cycle repeated 3 times. As can be seen from Figure 37, the diameter and count rate values stayed the same over the cycles.

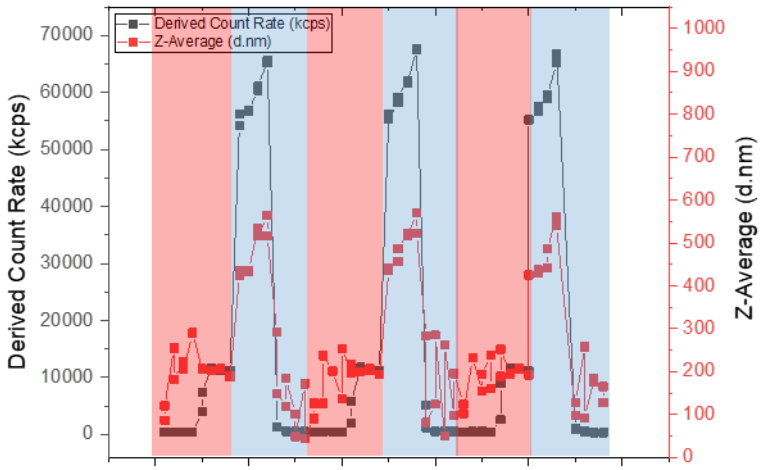

Figure 37. DLS curve for CMC-*g*-PNIPAM #2 (1 mg/mL in water). Red area – heating from 20 to 50 ˚C, blue area – cooling from 50 to 20 ˚C.

Figure 38 shows the DLS curves for the samples obtained by grafting PDEGMA via EDC/NHS chemistry and by grafting PNIPAM via click chemistry. The click chemistry samples showed thermal response similar to the samples with PNIPAM grafted via EDC/NHS chemistry. When PDEGMA was grafted on CMC and CNF, the phase change occurred at a lower temperature at around 25-30 °C.

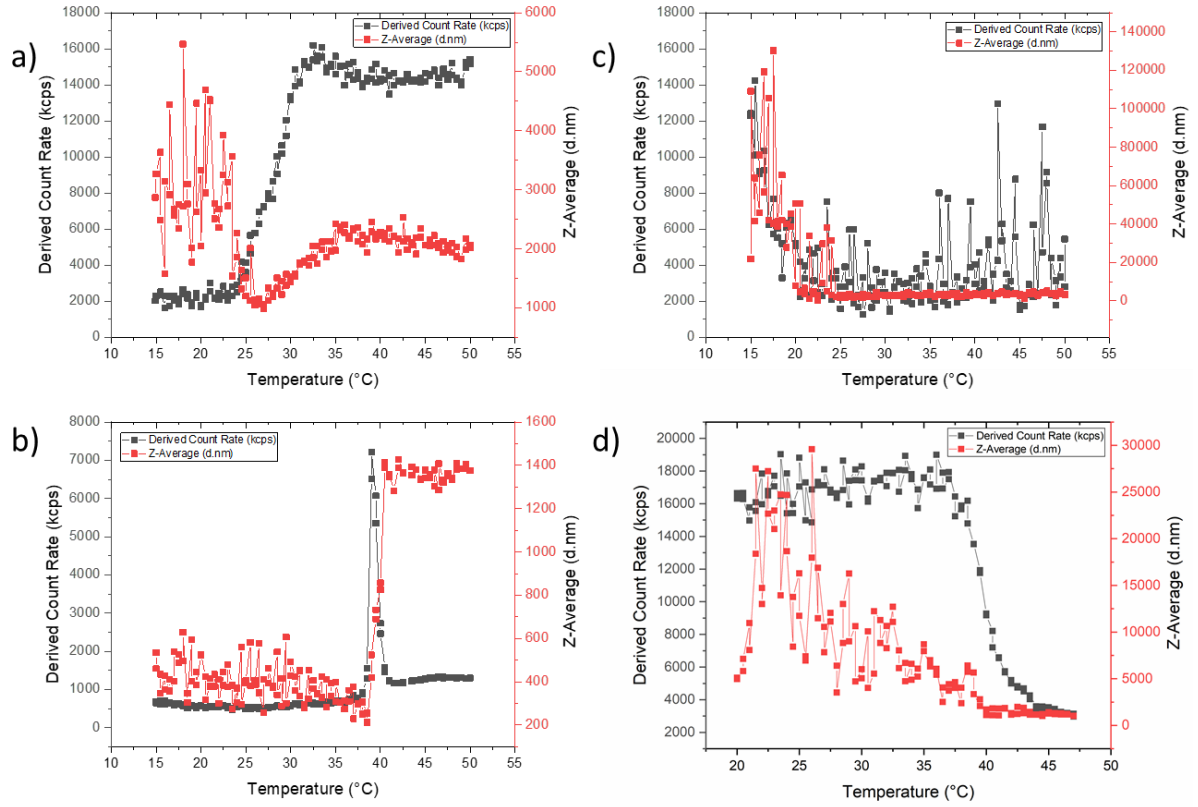

Figure 38. DLS curves for water solutions of a) CMC-*g*-PDEGMA (1 mg/mL), b) CMC-*g*-PNIPAM #click (1 mg/mL), c) CNF-*g*-PDEGMA #1 (never-dried, ~3 mg/mL), d) CNF-*g*-PNIPAM #click (never-dried, ~3 mg/mL).

In contrast with the PNIPAM- modified CMC and CNF, PDEGMA-modified cellulose hydrogels exhibited a phase change well below the human body temperature, but still higher than the room temperature. A few of the CMC/CNF-*g*-PNIPAM samples showed phase transition at 40 °C which would not be interesting for biomedical applications. Thus, by far it seems more beneficial to modify the celluloses with PDEGMA than with PNIPAM. However, if there was a way to slightly decrease the LCST of PNIPAM and PNIPAM- modified cellulose hydrogels, those would become potentially useful for biomedical industry as well.

4.8. Rheological properties of CMC and CNF graft copolymers

The rheological properties of the obtained hydrogels are criteria growing in importance as to judge their feasibility for potential biomedical applications. Unmodified and modified CMC hydrogels were chosen to conduct rheological tests. CNF samples were not selected as their concentration in water was too low for testing and it could not be altered without redispersion problems.

The strain amplitude dependence of the storage and loss moduli (G', G'') was measured to determine the linear viscoelastic region (LVE) of CMC or the critical strain level, until which the material's rheological properties are independent of strain. Figure 39 shows a strain sweep for CMC. The critical strain was determined to be around 20 %. Increasing the strain above this critical value disrupts the network structure.

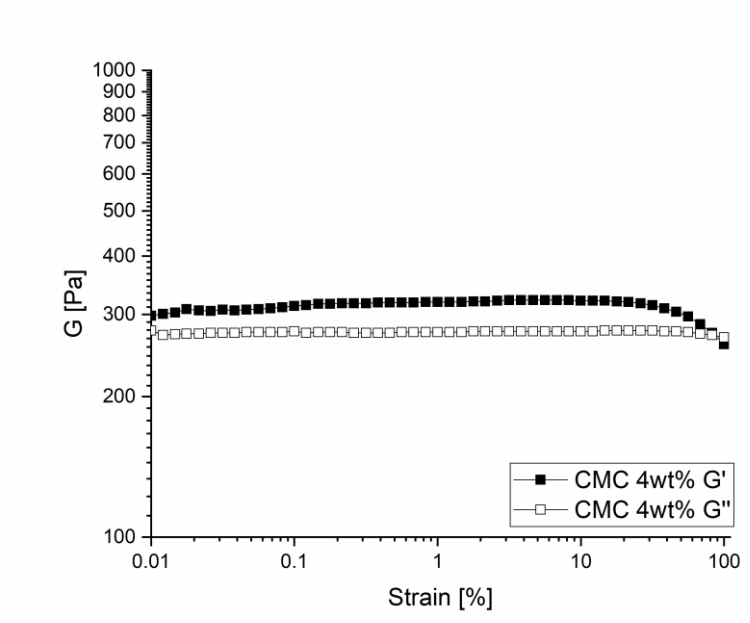

Figure 39. Strain sweep for a 4 wt% water solution of CMC.

After the CMC´s linear viscoelastic region has been defined by the strain sweep, its structure was further characterized using a frequency sweep at a strain far below the critical strain ensuring a linear response (here: 1 %). Figure 40 illustrates the frequency sweep results of 2 to 6-wt% CMC solutions at temperatures ranging from 20 to 50 °C. Regardless of the temperature and concentration, the storage moduli were lower than the loss moduli indicating for a viscous,

fluid-like behavior of aqueous CMC solutions. With an increasing concentration of CMC in the solution, both moduli showed higher values and the storage modulus almost became equal to loss modulus at 6 wt%. This indicates that 6 wt% is the critical concentration at which the material stops to flow. No significant change in the rheological behavior was observed when changing the temperature from 20 to 50 °C. Thus, no thermal response was observed in pure CMC solutions.

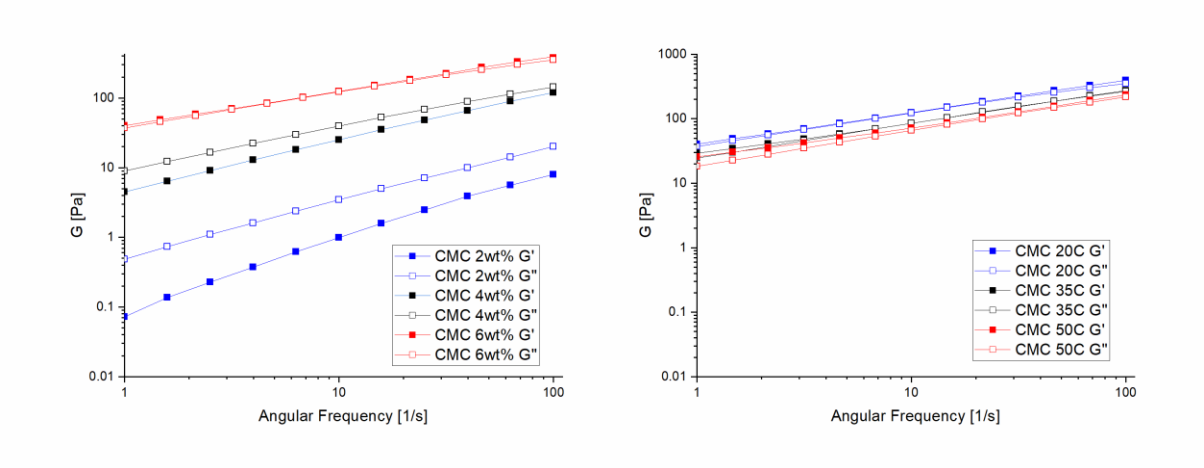

Figure 40. Frequency sweep on *(left)* 2-6 wt% water solutions of CMC at 20 °C, *(right)* 6 wt% water solutions of CMC at 20-50 °C.

Figure 41 presents the rheological behavior of CMC-*g*-PNIPAM #2 and #3 under and above the PNIPAM LCST. For both of the samples, the storage moduli were lower than the loss moduli at 20 °C. Upon heating to 50 °C, they switched and the loss moduli became greater than storage moduli. Thus, the samples show a more fluid-like behavior at 20 °C and more solid-like at 50 °C. This confirms physical crosslinking occurring at higher temperatures. This result is in agreement with the findings of Marques et al. (2006).[8] One of their PNIPAM- modified CMC samples showed thermos-thickening behavior, due to the intermolecular associations among the side chains that were initiated by heating. The viscosity of their 7 g/L CMC-*g*-PNIPAM water solution was notably higher at 60 °C than at 20 °C.

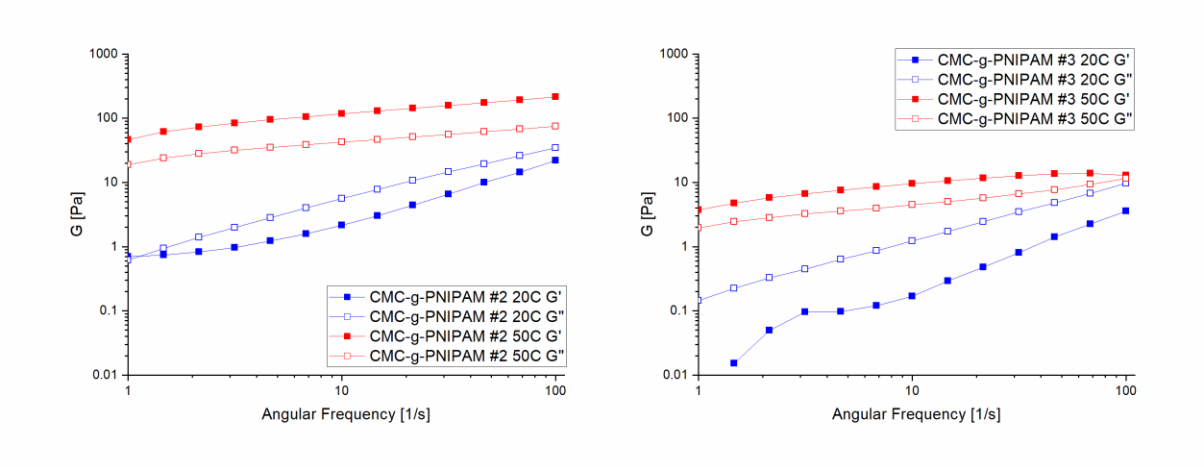

Figure 41. Frequency sweep on 6 wt% CMC-*g*-PNIPAM #2 and #3 at 20 and 50 ˚C.

5. CONCLUSION

Thermo-responsive bio-based hydrogels have promising potential in the field of biomedical applications. In this work, the feasibility of producing thermo-responsive cellulose hydrogels by grafting low-molecular-weight polymer chains was investigated. Firstly, azide- and amide-modified homopolymers of DEGMA and NIPAM were synthesized via ATRP. These polymers were grafted onto CMC and CNF via EDC/NHS-mediated cross-linking or a Cu-catalyzed alkyne-azide-click reaction, resulting in thermo-responsive cellulose-based hydrogels. ATR-IR spectroscopy, used to qualitatively characterize the cellulose-based graft co-polymers, demonstrated the presence of PNIPAM and PDEGMA in the modified CMC and CNF samples. However, it was not possible to distinguish between a covalent attachment of the polymer chains or physical adsorption on the cellulose carboxylate groups. PNIPAM has been confirmed to adsorb onto CMC and CNF forming stable complexes despite several purification methods. Nevertheless, the resulting hydrogels exhibited favorable thermal response in terms of their temperature dependence and rheological properties, as well as their transparency and size of the agglomerates. PNIPAM- and PDEGMA-modified cellulose hydrogels underwent a phase transition at around 35-40 °C and 25-30 °C, respectively. Based on these results, PDEGMA-modified cellulose hydrogels are more promising for potential biomedical applications since the whole temperature range for their LCSTs is above room temperature and below human body temperature. Some of the PNIPAM-modified cellulose samples demonstrated a phase change already at 35 °C, but for many of them the phase change occurred above human body temperature. If it would be possible to tune the phase change to below 36-37 °C, PNIPAM-modified cellulose hydrogels might be promising candidates for biomedical industry as well. The rheology experiments showed that physical crosslinking occurred in CMC-*g*-PNIPAM at 50 °C, changing the behavior of the hydrogel from liquid-like to solid-like. The obtained thermo-responsive bio-based hydrogels have promising potential in the field of biomedical applications for controlled delivery of drugs, proteins, or cells, and tissue engineering approaches.

6. FUTURE RESEARCH

It will be important that future research proves the chemical grafting of thermo-responsive polymers onto CMC and CNF. This may be explored by analyzing the samples for their elemental compositions and performing some NMR tests. Furthermore, it is desirable to investigate whether the resulting hydrogels are shear-thinning or shear-thickening. This may be done by measuring shear stress and viscosity of the samples as functions of shear rate. Concentric shape cylinder must be used in this case.

Another interesting topic for future work is tuning the LCST of the cellulose copolymers by changing the molecular weight of grafted PNIPAM and PDEGMA. One might also explore different grafting densities and their effect on the thermo-response of the copolymers. The minimum amount of added PNIPAM or PDEGMA necessary to keep a significant thermo-responsive behavior is especially of interest.

Click chemistry is very promising and so far, copper mediated azide/alkyne click chemistry (CuAAC) has been utilized the most. However, the thiol-ene click reaction does not require a metal catalyst, as compared with CuAAC. This reaction has already been successfully performed on native cellulose. [59] Hence, it might be interesting to try this method for grafting thermo-responsive polymer chains on CMC and CNF.

Thermo-responsive polymers may be grafted by targeting the hydroxylic groups available on the surface of cellulose. For instance, CNF can be modified by the esterification of 1-azido-2,3-epoxy-propane yielding amino functionalized cellulose which can be later “clicked” with an alkyne functionalized thermo-responsive polymer. [38]

Instead of using shear-thinning CMC and CNF, agarose might be used as a base of the hydrogel. Agarose is naturally shear-thickening due to chain bundling in a certain temperature range. Once modified with thermo-responsive polymers, agarose hydrogels might have both desirable properties: thermal response and shear-thickening behavior.

7. REFERENCES

1. Porsch, C., Hansson, S., Nordgren, N. & Malmström, E. Thermo-responsive cellulose-based architectures: Tailoring LCST using poly(ethylene glycol) methacrylates. *Polym. Chem.* (2011). doi:10.1039/c0py00417k
2. Larsson, E. *et al.* Thermo-responsive nanofibrillated cellulose by polyelectrolyte adsorption. *Eur. Polym. J.* (2013). doi:10.1016/j.eurpolymj.2013.05.023
3. Klemm, D., Heublein, B., Fink, H. P. & Bohn, A. Cellulose: Fascinating biopolymer and sustainable raw material. *Angew. Chem. Int. Ed.* (2005). doi:10.1002/anie.200460587
4. Shokri, J. & Adibkia, K. Application of Cellulose and Cellulose Derivatives in Pharmaceutical Industries. (2013).
5. Miyamoto, T., Takahashi, S., Ito, H., Inagaki, H. & Noishiki, Y. Tissue biocompatibility of cellulose and its derivatives. *J. Biomed. Mater. Res.* **23**, 125–133 (1989).
6. Vartiainen, J. *et al.* Health and environmental safety aspects of friction grinding and spray drying of microfibrillated cellulose. *Cellulose* **18**, 775–786 (2011).
7. Ni, C., Wang, W., Zhu, C., Huang, B. & Yao, B. Grafting polymerization of N-isopropylacrylamide on the surfaces of silica by ATRP and its application in HPLC. *Soft Mater.* (2010). doi:10.1080/15394451003598395
8. do Nascimento Marques, N., de Lima, B. & de Carvalho Balaban, R. Carboxymethylcellulose Grafted to Amino-Terminated Poly(N-isopropylacrylamide): Preparation, Characterization and Evaluation of the Thermoassociative Behaviour at Low Concentrations. *Macromol. Symp.* (2016). doi:10.1002/masy.201600004
9. Dufresne, A. Chapter 1. Cellulose and potential reinforcement. in *Nanocellulose: from nature to high performance tailored materials* (De Gruyter).
10. Eyley, S. & Thielemans, W. Surface modification of cellulose nanocrystals. *Nanoscale* (2014). doi:10.1039/c4nr01756k
11. Cumpstey, I. Chemical modification of polysaccharides. *Org. Chem.* (2013).
12. Heise, K. Chemical modification of lignocelluloses - their accessibility in selected reaction systems for the preparation of hydrogels, PhD diss. (Dresden University of Technology, 2017).
13. De France, K., Hoare, T. & Cranston, E. Review of Hydrogels and Aerogels Containing

Nanocellulose. *Chem. Mater.* (2017). doi:10.1021/acs.chemmater.7b00531

14. Guo, J. Covalent Modification of Nanocellulose Towards Advanced Functinal Materials, PhD diss. (Aalto University, 2017).
15. Saito, T., Kimura, S., Nishiyama, Y. & Isogai, A. Cellulose nanofibers prepared by TEMPO-mediated oxidation of native cellulose. *Biomacromolecules* (2007). doi:10.1021/bm0703970
16. Nippon Paper Industries Co., L. Cellulose nanofiber manufacturing technology and application development. *2018*
17. Turbak, A., Snyder, F. & Sandberg, K. Microfibrillated Cellulose, a New Cellulose Product: Properties, Uses, and Commercial Potential. in *Proceedings of the Ninth Cellulose. Applied Polymer Symposia 37. Conference.* (ed. N.Y.: Wiley.) 815–827 (1983).
18. Zimmermann, T., Pöhler, E. & Geiter, T. Cellulose Fibrils for Polymer Reinforcement. *Adv. Eng. Mater.* **6**, 754–761 (2004).
19. Siquera, G., Tapin-Lingua, S., Bras, J., da Silva Perez, D. & Dufresne, A. Morphological investigation of nanoparticles obtained from combined mechanical shearing, and enzymatic and acid hydrolysis of sisal fibers. *Cellulose* **17**, 1147–1158 (2010).
20. Pääkko, M. *et al.* Enzymatic hydrolysis combined with mechanical shearing and high-pressure homogenization for nanoscale cellulose fibrils and strong gels. *Biomacromolecules* (2007). doi:10.1021/bm061215p
21. Wågberg, L. *et al.* The build-up of polyelectrolyte multilayers of microfibrillated cellulose and cationic polyelectrolytes. *Langmuir* (2008). doi:10.1021/la702481v
22. Dufresne, A. Chapter 5. Chemical modification of nanocellulose. in *Nanocellulose: from nature to high performance tailored materials* (De Gruyter). doi:10.1515/9783110254600.147
23. Lavoine, N., Bras, J., Saito, T. & Isogai, A. Optimization of preparation of thermally stable cellulose nanofibrils via heat-induced conversion of ionic bonds to amide bonds. *J. Polym. Sci. Part A Polym. Chem.* (2017). doi:10.1002/pola.28541
24. Wei, J. *et al.* Thermo-responsive and compression properties of TEMPO-oxidized cellulose nanofiber-modified PNIPAm hydrogels. *Carbohydr. Polym.* (2016). doi:10.1016/j.carbpol.2016.04.015
25. Missoum, K., Belgacem, M. N. & Bras, J. Nanofibrillated cellulose surface modification: A review. *Materials (Basel).* (2013). doi:10.3390/ma6051745
26. Guo, J. Covalent Modification of Nanocellulose Towards Advanced Functinal

Materials. (Aalto University, 2017).

27. Filpponen, I. & Rojas, O. Surface modification of forest biomaterials. (Aalto University, 2015).
28. Blomstedt, M. Modification of cellulosic fibers by carboxymethyl cellulose - effects on fiber and sheet properties. (2017).
29. Hermanson, G. Chapter 4. Zero-Length Crosslinkers. in *Bioconjugate Techniques* 259–273 (2013).
30. Thambi, T., Phan, V. H. G. & Lee, D. S. Stimuli-Sensitive Injectable Hydrogels Based on Polysaccharides and Their Biomedical Applications. *Macromolecular Rapid Communications* (2016). doi:10.1002/marc.201600371
31. Thermo Fischer Scientific. Carbodiimide Crosslinker Chemistry.
32. Conzatti, G., Ayadi, F., Cavalie, S., Carrère, N. & Tourrette, A. Thermosensitive PNIPAM grafted alginate/chitosan PEC. *Appl. Surf. Sci.* (2019). doi:10.1016/j.apsusc.2018.10.269
33. Fang, J., Chen, J., Leu, Y. & Hu, J. Temperature-sensitive hydrogels composed of chitosan and hyaluronic acid as injectable carriers for drug delivery. *Eur. J. Pharm. Biopharm.* **68**, 626–636 (2008).
34. do Nascimento Marques, N., de Lima, B. L. B. & de Carvalho Balaban, R. Carboxymethylcellulose Grafted to Amino-Terminated Poly(N-isopropylacrylamide): Preparation, Characterization and Evaluation of the Thermoassociative Behaviour at Low Concentrations. *Macromol. Symp.* (2016). doi:10.1002/masy.201600004
35. Kolb, H., Finn, M. & Sharpless, K. Click Chemistry : Diverse Chemical Function from a Few Good Reactions. *Angew. Chem* **40**, 2004–2021 (2001).
36. Iha, R. *et al.* Applications of orthogonal 'Click' Chemistries in the synthesis of functional soft materials. *Chem. Rev.* (2009). doi:10.1021/cr900138t
37. Bao, H. *et al.* Thermo-and pH-responsive association behavior of dual hydrophilic graft chitosan terpolymer synthesized via ATRP and click chemistry. *Macromolecules* (2010). doi:10.1021/ma100894p
38. Pahimanolis, N. *et al.* Surface functionalization of nanofibrillated cellulose using click-chemistry approach in aqueous media. *Cellulose* (2011). doi:10.1007/s10570-011-9573-4
39. Bao, H.; Li, L.; Leong, W.C.; Gan, L. H. Thermo-responsive association of chitosan-graft-poly(N-isopropylacrylamide) in aqueous solutions hongqian. *J. Phys. Chem.* **114**, 10666–10673 (2010).

40. Li, X.; Yuan, W.; Gu, S.; Ren, J. Synthesis and self-assembly of tunable thermosensitive chitosan amphiphilic copolymers by click chemistry. *Mater. Lett.* **64**, 2663–2666 (2010).
41. Yuan, W.; Li, X.; Gu, S.; Cao, A.; Ren, J. Amphiphilic chitosan graft copolymer via combination of ROP, ATRP, and click chemistry: Synthesis, self-assembly, thermosensitivity, fluorescence, and controlled drug release. *Polymer (Guildf).* **52**, 658–666 (2010).
42. Zhang, J., Xu, X., Wu, D., Zhang, X. & Zhuo, R. Synthesis of thermosensitive P(NIPAAm-co-HEMA)/cellulose hydrogels via 'click' chemistry. *Carbohydr. Polym.* (2009). doi:10.1016/j.carbpol.2009.01.023
43. Joubert, F., Musa, O., Hodgson, D. & Cameron, N. Graft copolymers of hydroxyethyl cellulose by a 'grafting to' method:15N labelling as a powerful characterisation tool in 'click' polymer chemistry. *Polym. Chem.* (2015). doi:10.1039/c4py01413h
44. Syverud, K., Pettersen, S., Draget, K. & Chinga-Carrasco, G. Controlling the elastic modulus of cellulose nanofibril hydrogels - scaffolds with potential in tissue engineering. *Cellulose* (2015). doi:10.1007/s10570-014-0470-5
45. Teotia A.K., Sami, H. & Kumar, A. Thermo-responsive polymers. in *Switchable and Responsive Surfaces and Materials for Biomedical Applications* (ed. Johnathan Zhang) 3–43 (Woodhead Publishing, 2015).
46. Hoogenboom, R. Temperature-responsive polymers: properties, synthesis and applications. in *Smart Polymers and their Applications* (Woodhead Publishing, 2014).
47. Cardoso, V., Ribeiro, C. & Lanceros-Mendez, S. Bioinspired Materials for Medical Applications. in 69–99 (Woodhead Publishing, 2017).
48. Pamies, R., Zhu, K., Kjøniksen, A. & Nyström, B. Thermal response of low molecular weight poly-(N-isopropylacrylamide) polymers in aqueous solution. *Polym. Bull.* (2009). doi:10.1007/s00289-008-0029-4
49. Vihola, H., Laukkanen, A., Valtola, L., Tenhu, H. & Hirvonen, J. Cytotoxicity of thermosensitive polymers poly(N-isopropylacrylamide), poly(N-vinylcaprolactam) and amphiphilically modified poly(N-vinylcaprolactam). *Biomaterials* (2005). doi:10.1016/j.biomaterials.2004.09.008
50. Lutz, J. Polymerization of oligo(ethylene glycol) (meth)acrylates: Toward new generations of smart biocompatible materials. *J. Polym. Sci. Part A Polym. Chem.* **46**, 3459–3470 (2008).
51. Cobo Sánchez, C. *Modification of nanofibrillated cellulose with stimuli-responsive*

polymers.

52. Gicquel, E., Martin, C., Heux, L., Jean, B. & Bras, J. Adsorption versus Grafting of Poly(N-Isopropylacrylamide) in aqueous conditions on the Surface of Cellulose Nanocrystals. *Carbohydr. Polym.* (2019). doi:10.1016/j.carbpol.2019.01.022
53. Conzatti, G. *et al.* PNIPAM grafted surfaces through ATRP and RAFT polymerization: Chemistry and bioadhesion. *Colloids and Surfaces B: Biointerfaces* (2017). doi:10.1016/j.colsurfb.2016.12.007
54. Matyjaszewski, K. & Xia, J. Atom Transfer Radical Polymerization. *Chem. Rev.* **101**, 2921–2990 (2001).
55. Appel, E., del Barrio, J., Loh, X. J., Dyson, J. & Scherman, O. High Molecular Weight Polyacrylamides by ATRP: Enabling Advancements in Water-based Applications. *J. Polym. Sci. part A* **50**, 181–186 (2012).
56. Sigma-Aldrich. ATRP: Complete Tools for the Synthesis of Well-Defined Functionalized Polymers. Available at: https://www.sigmaaldrich.com/materials-science/polymer-science/atrp.html.
57. Matyjaszewski Polymer Group. Carnegie Mellon University: Fundamentals of an ATRP reaction. Available at: https://www.cmu.edu/maty/index.html.
58. Socrates, G. *Infrared and Raman Characteristic Group Frequencies. Tables and Charts.* (2001).
59. Zhao, G., Hafrén, J., Deiana, L. & Córdova, A. Heterogeneous ‘“Organoclick”’ Derivatization of Polysaccharides: Photochemical Thiol-ene Click Modification of Solid Cellulose a. doi:10.1002/marc.200900764

8. APPENDIX

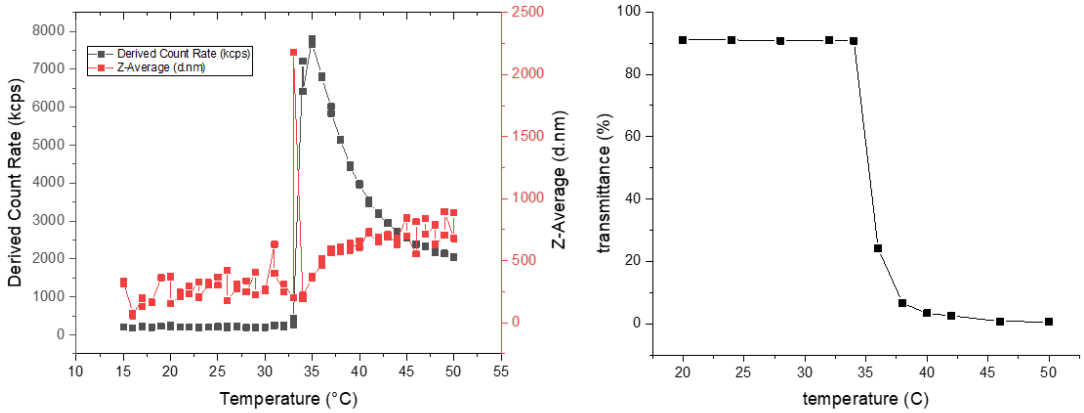

Appendix 1. *(Left)* DLS and *(right)* UV-VIS transmittance at 500 nm of PNIPAM-NH_2 (Sigma Aldrich) water solution (1 mg/mL).

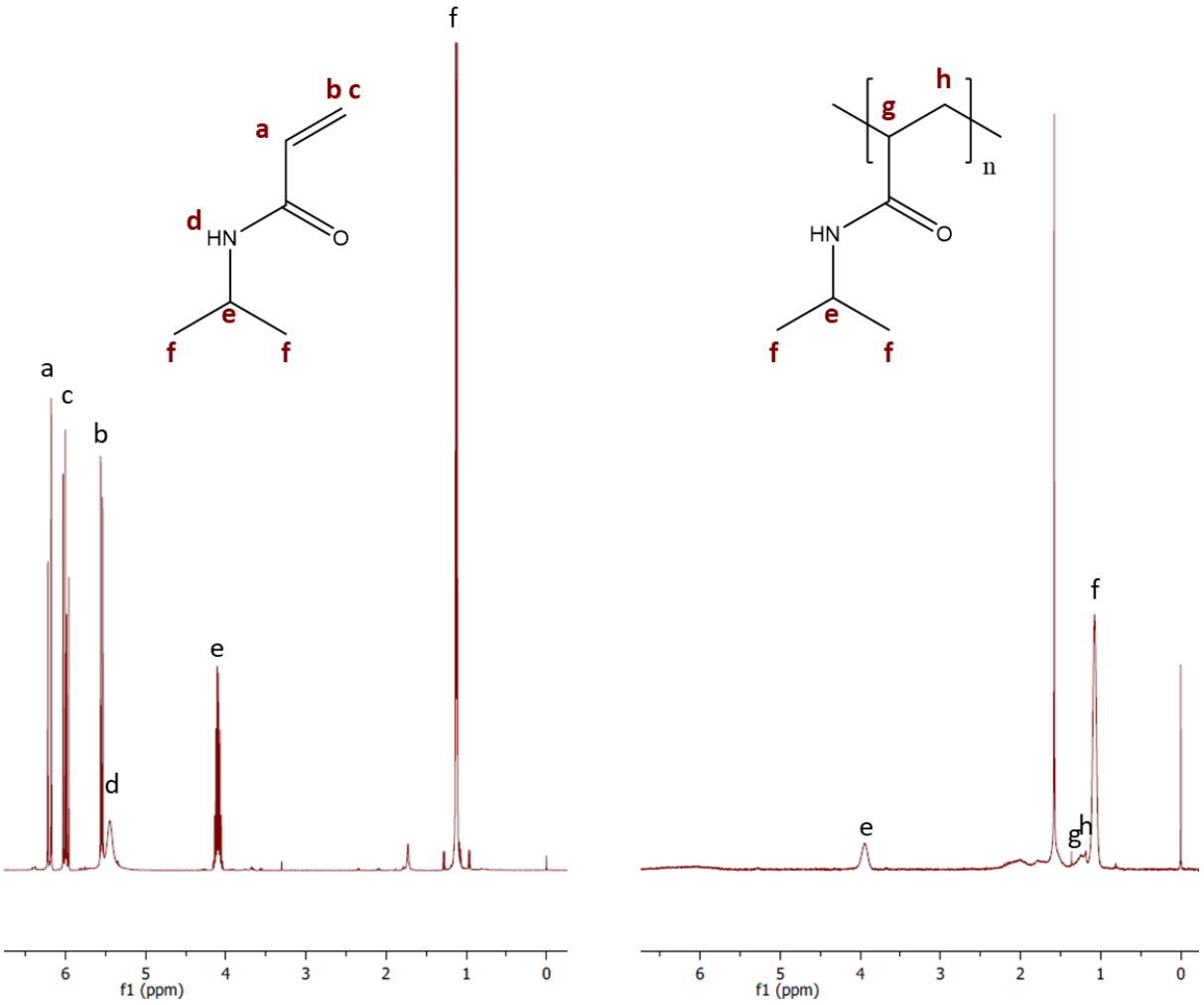

Appendix 2. ^{1}H NMR spectra in $CDCl_3$ at RT – *(left)* NIPAM monomer and *(right)* PNIPAM-*Cl* polymer after dialysis.

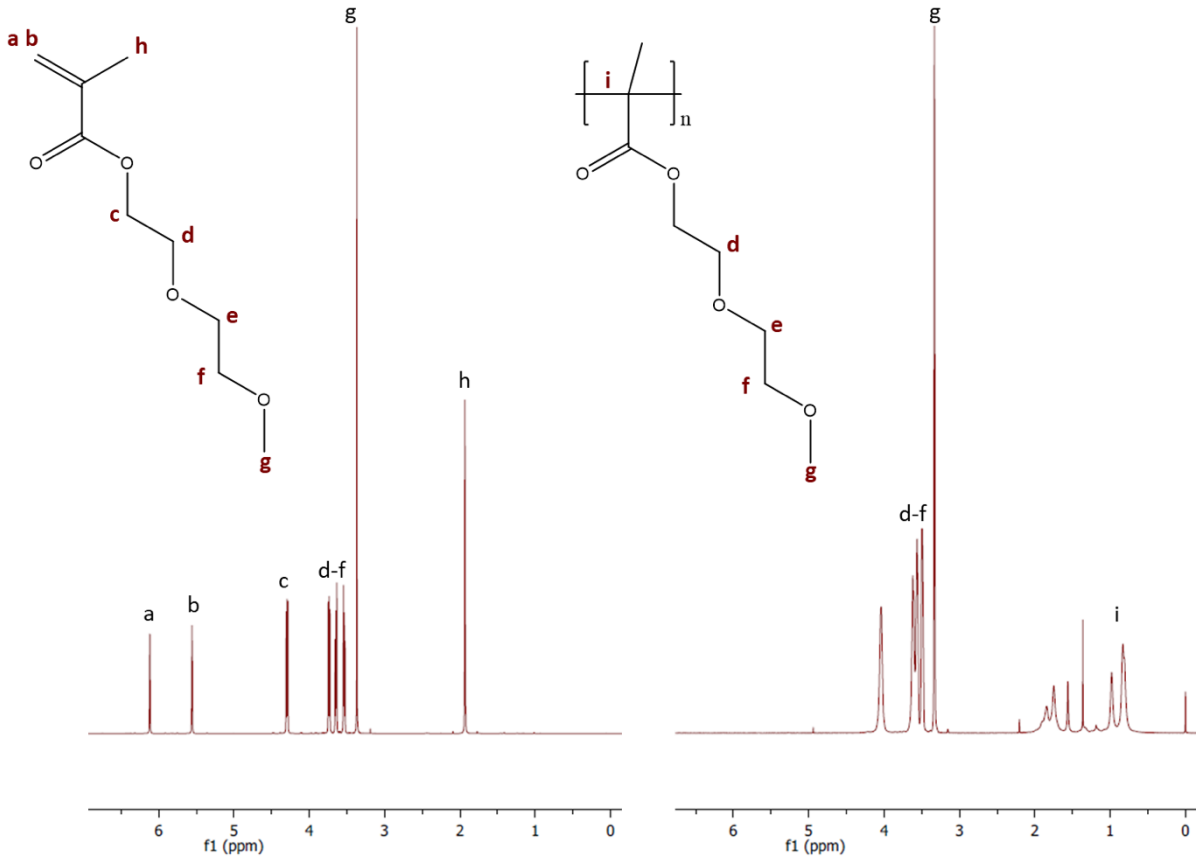

Appendix 3. ^{1}H NMR spectra in $CDCl_3$ at RT – *(left)* DEGMA monomer and *(right)* PDEGMA-*NH_2* #1 polymer after dialysis.

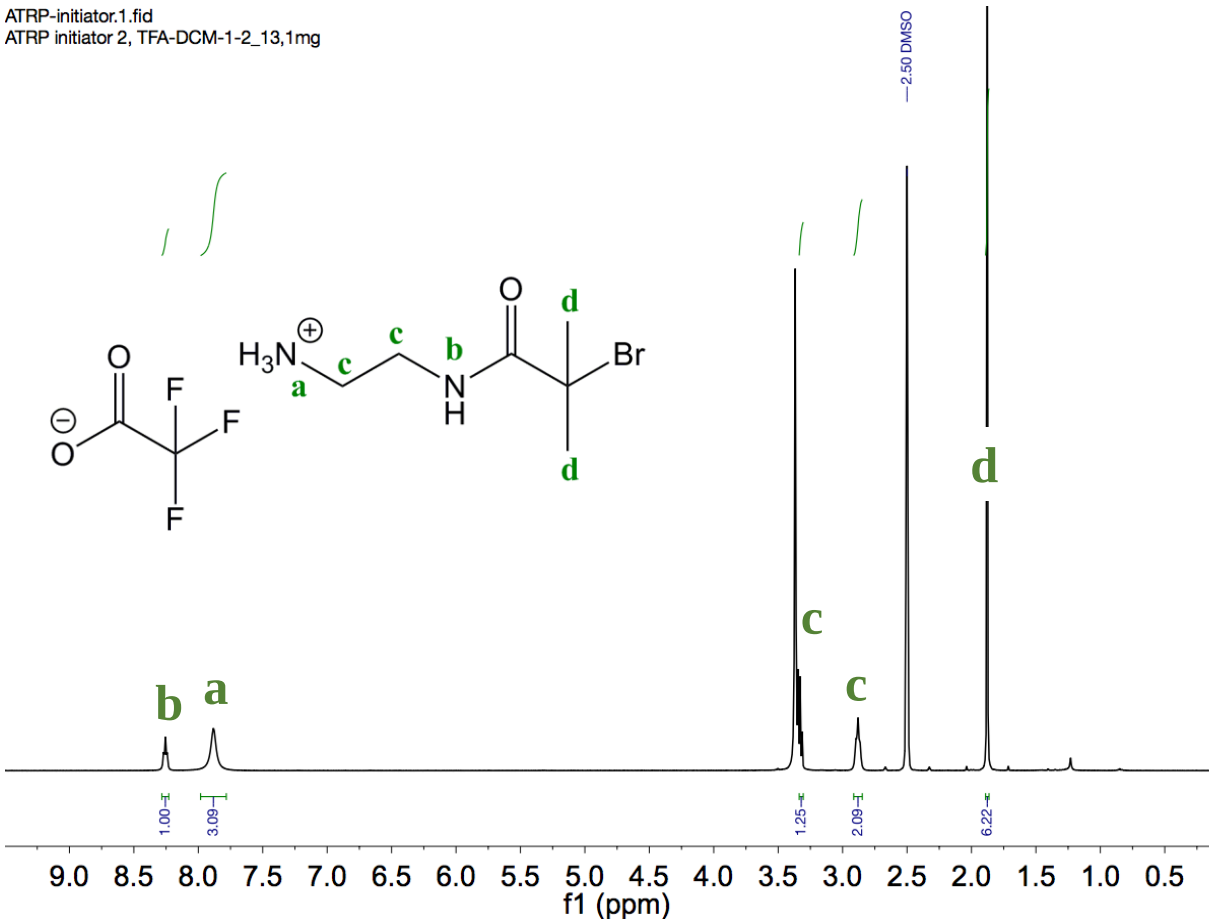

Appendix 4. ^{1}H NMR spectrum of the NH_2-terminated ATRP initiator (BIBB-*NH_2*) in DMSO-d_6 at RT.